AD-A125 181 BASIC PROBLEMS IN INP TECHNOLOGY(U) HUGHES RESEARCH LABS MALIBU CA K V VAIDYANATHAN ET AL. NOV 82 AFOSR-TR-82-1100 F49620-81-C-0037 1/1

UNCLASSIFIED F/G 20/12 NL

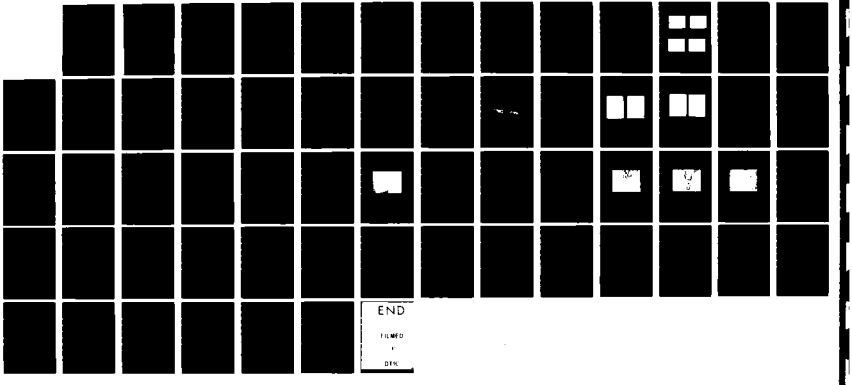

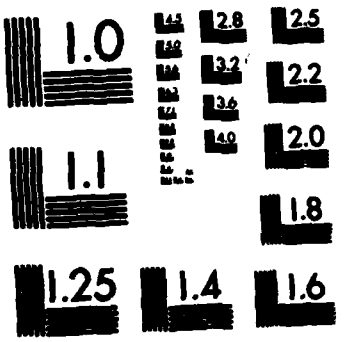

AFOSR-TR- 82-1100

BASIC PROBLEMS IN InP TECHNOLOGY

K. V. Vaidyanathan

Hughes Research Laboratories
3011 Malibu Canyon Road
Malibu, CA 90265

November 1982

F49620-81-C-0037
Final Report
Period From 28 February 1981 through 27 February 1982

AFOSR/NE
Director of Electronic and Material Sciences
Building 410
Bolling AFB, DC 20332

UNCLASSIFIED

SECURITY CLASSIFICATION OF THIS PAGE (When Data Entered)

REPORT DOCUMENTATION PAGE	READ INSTRUCTIONS BEFORE COMPLETING FORM
1. REPORT NUMBER: AFOSR-TR- 82-1100	2. GOVT ACCESSION NO.: AD-A125 181	3. RECIPIENT'S CATALOG NUMBER
4. TITLE (and Subtitle): BASIC PROBLEMS IN InP TECHNOLOGY	5. TYPE OF REPORT & PERIOD COVERED: Final Report; Feb. 28, 1981 Feb. 27, 1982
	6. PERFORMING ORG. REPORT NUMBER
7. AUTHOR(s): K.V. Vaidyanathan and H.L. Dunalp	8. CONTRACT OR GRANT NUMBER(s): F49620-81-C-0037
9. PERFORMING ORGANIZATION NAME AND ADDRESS: Hughes Aircraft Company, Hughes Research Laboratories, 3011 Malibu Canyon Road, Malibu, CA 90265	10. PROGRAM ELEMENT, PROJECT, TASK AREA & WORK UNIT NUMBERS: 2306/B2 61102F
11. CONTROLLING OFFICE NAME AND ADDRESS: AFOSR/NE, Director of Electronic and Material Sciences, Building 410, Bolling AFB, DC 20332	12. REPORT DATE: Nov 1982
	13. NUMBER OF PAGES: 59
14. MONITORING AGENCY NAME & ADDRESS(if different from Controlling Office)	15. SECURITY CLASS. (of this report): UNCLASSIFIED
	15a. DECLASSIFICATION DOWNGRADING SCHEDULE

16. DISTRIBUTION STATEMENT (of this Report)

Distribution unlimited.

Approved for public release; distribution unlimited.

17. DISTRIBUTION STATEMENT (of the abstract entered in Block 20, if different from Report)

18. SUPPLEMENTARY NOTES

19. KEY WORDS (Continue on reverse side if necessary and identify by block number)

Ion implantation doping of InP; Surface preparation of InP; Annealing of InP; Determination of iron in InP; Redistribution of Fe in InP during thermal processing

20. ABSTRACT (Continue on reverse side if necessary and identify by block number)

Procedures for evaluating the thermal stability of semi-insulating InP have been developed. The determination of the concentration of iron in S.I. InP and the migration of Fe during high temperature processing have been identified as a major problem. The effectiveness of plasma deposited Si_3N_4 and chemical vapor deposited phosphosilicate glass (PSG) as annealing encapsulants have been evaluated. PSG appears to be the encapsulant of choice at the moment.

DD FORM 1 JAN 73 1473 EDITION OF 1 NOV 65 IS OBSOLETE

UNCLASSIFIED

SECURITY CLASSIFICATION OF THIS PAGE (When Data Entered)

Beryllium is a well behaved acceptor in InP. It can be activated at quite low temperatures (∿525°C). Preliminary secondary ion mass spectrometry studies show that at high concentrations beryllium exhibits a high diffusion coefficient. Among the donor dopants studied, silicon, germanium, tin, and selenium are all well behaved. In the case of heavier mass dopants, implanting at an elevated temperature (150°C) increases the electrical activation efficiency. None of these dopants diffuse significantly during high temperature annealing.

TABLE OF CONTENTS

LIST OF ILLUSTRATONS

SECTION 1

INTRODUCTION

A. ADVANTAGES OF InP

Both InP and the ternary InGaAs have electronic properties which make them attractive for high speed microwave and opto-electronic device applications. For example, both of these materials exhibit considerably higher steady-state electron velocities at all values of electric fields than silicon. It is possible to grow $In_{0.53}Ga_{0.47}As$ epitaxial layers lattice-matched to InP. At this composition of the ternary alloy, photodetectors capable of detecting 1.6 μm have been fabricated. In this wavelength range low loss, low dispersion, radiation-resistant fibers are available, making these materials attractive for fiber optic applications. The unique properties of InP that make it attractive for high speed device applications are discussed below.

The electron velocity-electric field characteristics of silicon, gallium arsenide, and indium phosphide are shown in Figure 1. An inspection of this curve shows that at low fields (<0.6 V/μm) electrons in GaAs exhibit higher velocities than those in Si or InP. However, at higher fields (0.7 V to 2.3 V/μm) InP is clearly superior to either GaAs or Si. Also, the curves in Figure 1 represent steady-state values, and for them to be valid the following conditions must be satisfied: (1) the applied field should be constant over distances that are long compared to the optical phonon-scattering mean free path, and (2) the applied voltage across the region of constant field should be substantially greater than the energy difference between the direct and indirect conduction band minima ($\Delta E_{\Gamma L}$). Violation of these conditions leads to the phenomenon of "velocity overshoot." Such overshoot can result in carriers reaching substantially higher velocities than steady-state for a particular value of electric field. For practical Si and GaAs devices, both conditions are satisfied for fields higher than 0.3 V/μm. In the case of InP, condition (2) may not be

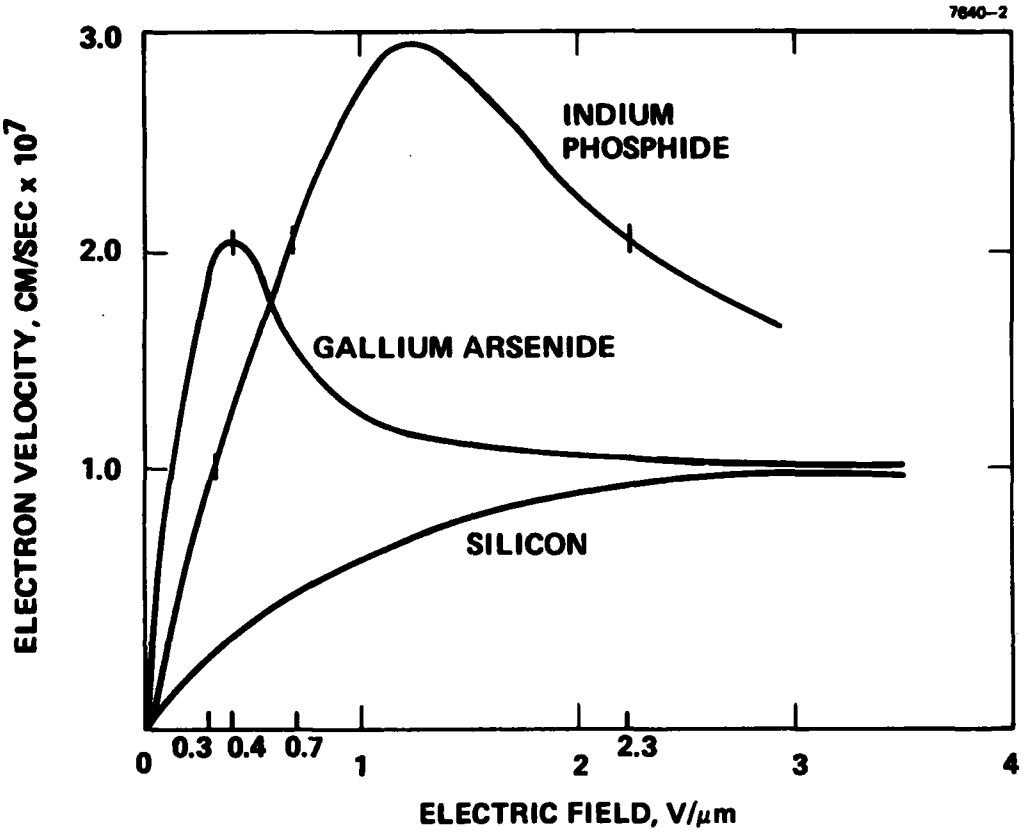

Figure 1. Electronic velocity versus electric field characteristics for Si, GaAs, and InP under steady-state conditions.

satisfied until a field of 0.7 V/μm is reached. Thus velocity overshoot effects may dominate in InP even at fields as high as 0.7 V/μm.

Another major advantage of InP is the ability to form a stable dielectric – semiconductor interface and the ability to fabricate metal insulator semiconductor field effect transistors (MISFETs). Such devices can sustain several volts of forward bias. In contrast, GaAs MESFET devices employing Schottky gates are limited to very small forward voltage swings. This feature relaxes the threshold voltage control requirements of individual devices for integrated circuit applications. We believe that this technology will be extremely useful in fabricating low power, high speed random access memories (RAMs).

As a result of this technology development program, we have established a reliable implantation and annealing process technology to form n^+ regions in InP. The results from this program have been used to fabricate discrete InP MISFET devices and integrated circuits employing such devices. The development and fabrication of devices and circuits were performed under Hughes internal research and develoment programs and a NOSC sponsored IC program, respectively. The discrete MISFETs with implanted source and drain dregions had a channel length of ~1.5 μm and a gate length of ~5 μm. The current-voltage characteristics of such a device are shown in Figure 2. Under a NOSC contract to demonstrate IC operation of MSI coplexity employing InP MISFETs, we have demonstrated a 15-stage ring oscillator with implanted load resistors and enhancement mode transistors. These circuits operated with a gate delay of 120 psec. Typical results are shown in Figure 3. These encouraging results have been made possible because of the process technology developments achieved under this contract and our IR&D programs.

The electronic properties of InGaAs also make it attractive for opto-electronic device applications. Photodetectors capable of operating at 1.6 μm can be fabricated on lattice-matched

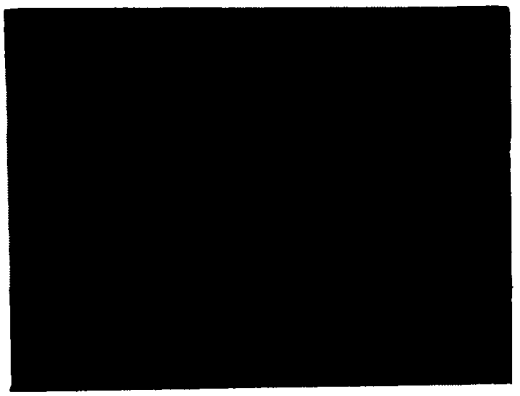

Figure 2(a).
Photograph of a planar InP MISFET with chahnel length of 1.5 μm.

11284-1R1

Figure 2(b).
I_D versus $_D$ characteristics for a InP E-MISFET.

11284-11

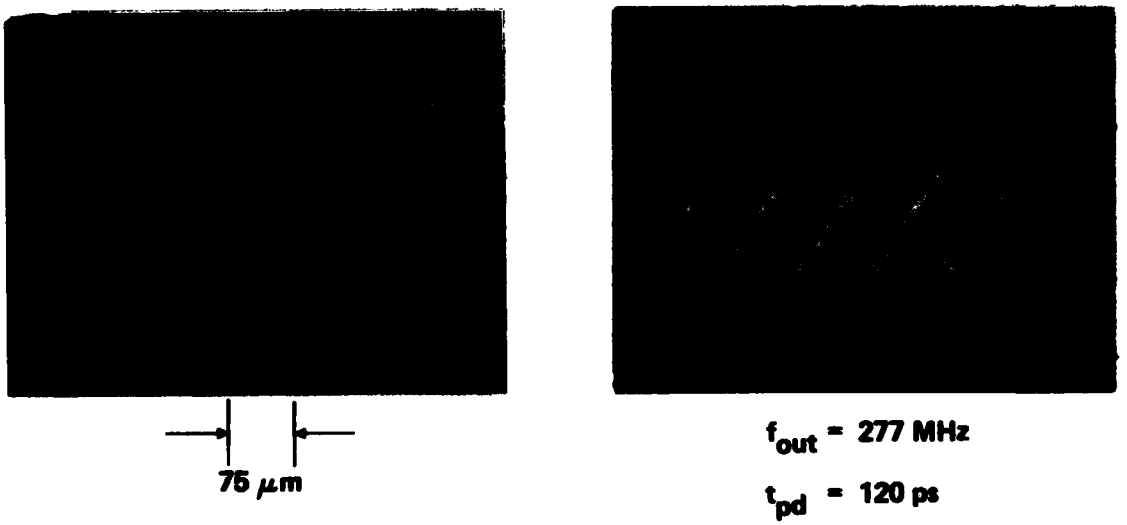

Figure 3. InP MISFET 15-stage ring oscillator.

InGaAs layers grown on InP. This wavelength range is of great interest in fiber optic communication systems because of the availability of radiation resistant, low loss, low dispersion optical fibers. The mutually compatible InGaAs/InP, InGaAsP/InP system makes it possible to integrate sources, detectors, and high speed signal processing elements and thus develop intelligent opto-electronic integrated circuits.

In this report, we discuss the major areas of investigation carried out in the program.

- In the area of epitaxial growth, we have demonstrated that high-purity, epitaxial layers with device-quality surface morphology can be grown using our infinite solution growth technique. We have investigated the influence of residual donors in InP such as silicon and sulfur and the control of the concentration of such impurities in the epitaxial layers by the introduction of water vapor in the growth ambient and by prolonged bake-out procedures, respectively. We have modified the system which will minimize thermal surface degradation of InP substrates prior to epitaxial layer growth.

- We have developed empirical procedures for evaluating the thermal stability of semi-insulating InP. This investigation clearly shows that quantitative determination of the iron content in semi-insulating InP and the migration of this deep level dopant during high temperature processing are the two problem areas to be studied.

- We have investigated procedures for encapsulating ion-implanted InP with an appropriate dielectric during the annealing process. These include the evaluation of a plasma-enhanced deposited silicon nitride and phosphosilicate glass (PSG) for encapsulation purposes.

- We have studied the electrical activation as well as atomic distribution of silicon, sulfur, carbon, selenium (donors) and beryllium (acceptor) implanted layers as a function of anneal parameters in InP. More detailed evaluations of the implanted dopants and defects present in the material will form the focal point for future investigations.

This report discusses the progress in these areas in detail.

SECTION 2

EPITAXIAL GROWTH OF InP

InP, (In, Ga)As, and (In, Ga)(As, P) layers can be epitaxially grown by a variety of techniques such as liquid-phase epitaxy (LPE),[1] vapor phase epitaxy (VPE),[2] metal organic chemical vapor deposition (MOCVD),[3] planar reactive deposition (PRD),[4] and molecular beam epitaxy (MBE).[5] It appears that LPE offers the best potential for the growth of high-purity InP at this stage.

Two variations of the LPE technique are commonly used: the slide-bar technique using small solutions (the limited melt technique) and the dipping technique using larger solutions (the infinite solution technique). The slide-bar technique has a disadvantage that severe melt depletion effects can occur. Consequently, only a few layers with reproducible properties can be grown from a single melt. This may be a potential problem in the growth of ternary and quaternary layers. In contrast, the infinite solution technique, in principle, permits several hundred layers with reproducible properties to be grown from the same melt.

Hughes Research Laboratories (HRL) has developed a system which allows us to use a large solution to grow the epitaxial layers. The system illustrated in Figure 1, consists basically of an all-quartz growth tube connected by a high-vacuum valve to a stainless-steel entry chamber. A saturated solution of the appropriate elements contained in a crucible serves as the growth matrix. Once a specific solution has been prepared, it is kept in a paladium-purified hydrogen ambient and can be maintained at or near the growth temperature in a controlled environment for months. During a long series of runs, all operations, such as adding dopants or introducing substrates for epi-growth, are performed by passing these materials through an entry chamber, which can be independently evacuated and flushed with hydrogen before

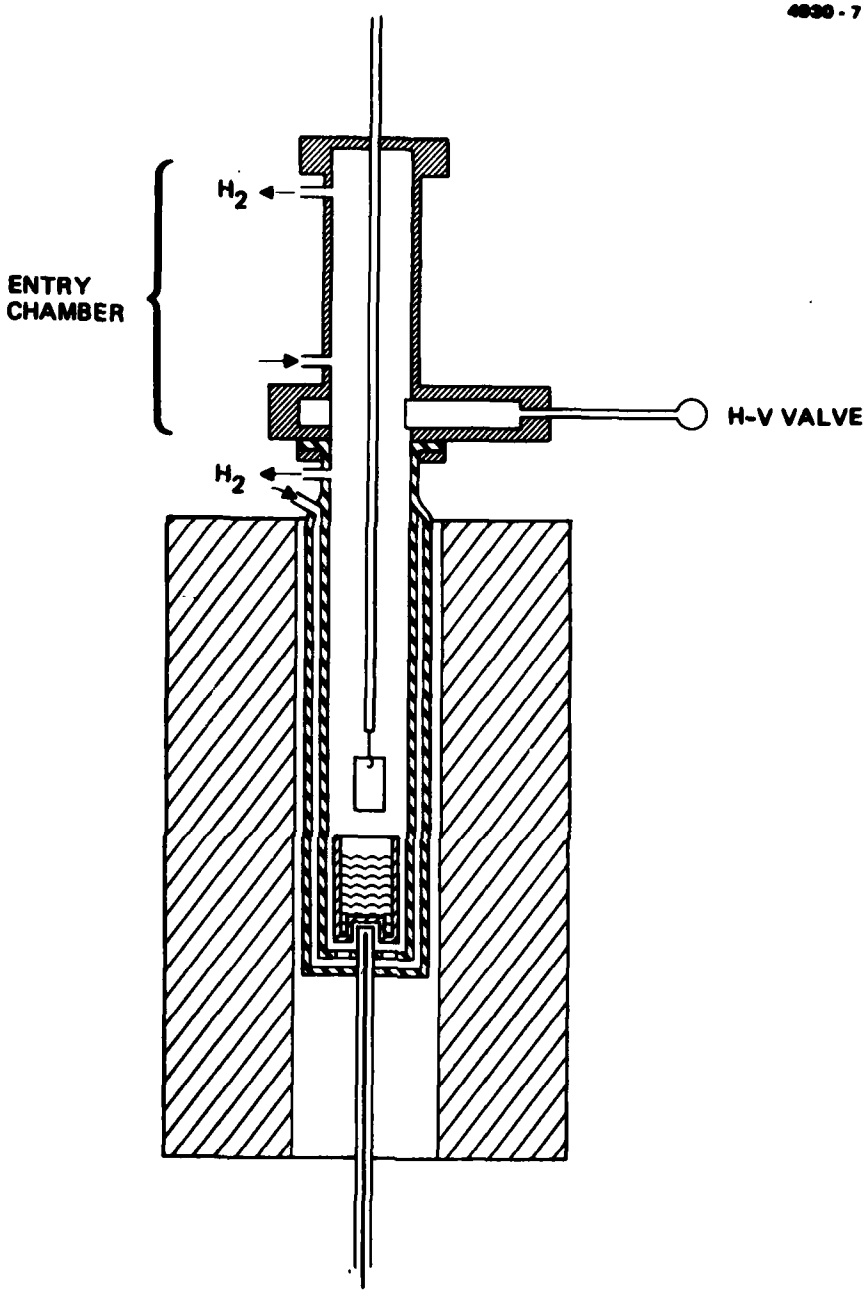

Figure 4. Schematic of LPE growth system.

opening to the growth tube. It is also possible to maintain any other appropriate growth ambient while keeping all other variables under control. This capability is extremely useful in the growth of high purity InP layers and is discussed in detail later in this section.

The performance of opto-electronic devices depends critically on the ability to grow uniform, thin, homogeneous and dislocation-free epitaxial layers. Also, in devices involving heterojunctions, it is necessary to reduce defects at the interface. To satisfy all of these requirements, the surfaces must see a uniform growth ambient (a chemically homogeneous growth matrix and uniform temperature over the growth surface), and the layers must be grown slowly enough to permit near-equlibrium conditions to be established at the growth interface.

We have developed a graphite sample holder assembly to house the substrate (Figure 5) that permits us to grow the layers under such conditions. The substrate is introduced into the melt within the sample holder, and the whole assembly rotates in the melt until temperature equilibrium is fully established. This rotation further helps to ensure good mixing and homogeneity in the melt. By raising the graphite cover, the sample is exposed to the melt. Growth is stopped by (1) closing the cover, (2) raising the sample holder out of the solution, and (3) reopening the cover, at which point the solution that is trapped in the sample holder falls out. Note that at no time in the growth procedure does the surface of the sample pass through the meniscus on the solution. Furthermore, the cover of the sample holder does not wipe the melt from the sample. Using this technique, we have grown thin epitaxial layers with excellent surface morphology and reproducible electrical properties.

The infinite solution technique has been successfully used to grow high-purity InP layers with carrier concentrations of ~3 x 10^{15} cm and mobilities of 4,500 $cm^2\ V^{-1}\ sec^{-1}$ (77°K mobility of 41,000 $cm^2\ V^{-1}\ sec^{-1}$) reproducibly. We have also conducted

extensive studies, using internal funds, to study the influence of ~0.1 to 10 ppm of water vapor in the growth ambient. The results of this study, summarized in Table 1, are qualitative in nature. They provide a good overall picture of the influence of water vapor in the growth ambient but are not quantitative. These results can be explained as follows. Silicon is believed to be the dominant residual donor in InP. The quartz in the growth system reacts with H_2, which reduces it to SiO vapor, which is then reduced by In in solution, resulting in Si doping of the solution. Consequently, in the presence of pure H, the Si level in solution reaches an equilibrium level. However, when a small quantity of water vapor is added to the growth ambient, the reduction of quartz by H is suppressed; also, the Si in solution reacts with water vapor, forming SiO vapors.

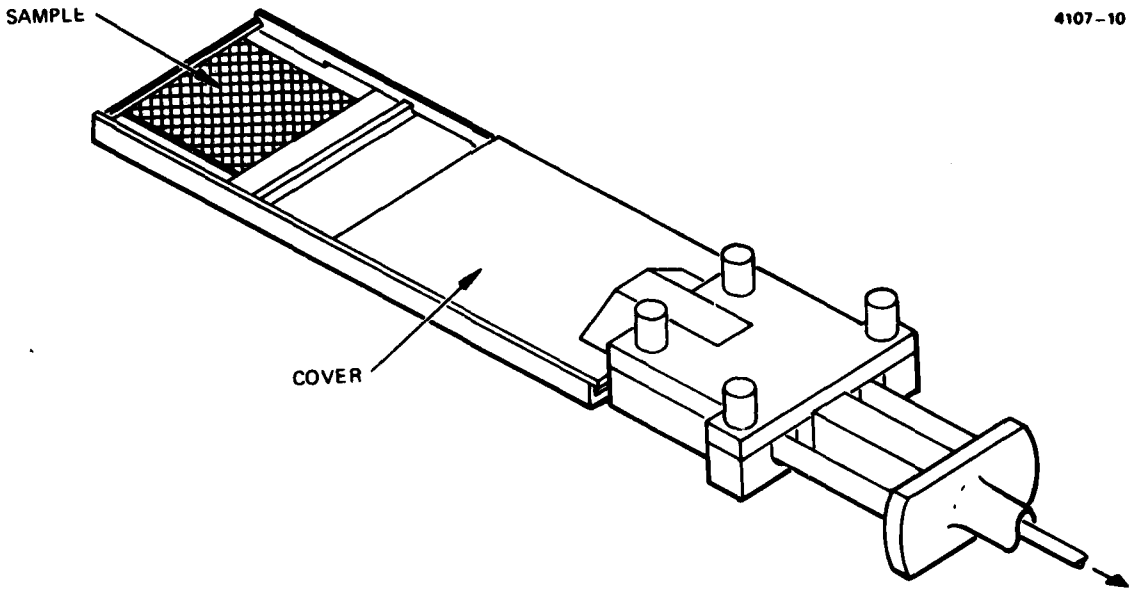

Figure 5. Graphite sample holder assembly.

Table 1. Electrical Properties of InP Epitaxial Layers Illustrating the Influence of Water Vapor in the Gas Stream

Sample Number	Ambient	n, cm^{-3} (300°K)	μ, $cm^2 V^{-1} sec^{-1}$ (300°K)
1	Pure hydrogen	1.4×10^{17}	2600
2	Pure hydrogen	2.6×10^{17}	2600
3	Hydrogen + H_2O	2.1×10^{15}	3500
4	Hydrogen + H_2O	2.3×10^{15}	4500
5	Hydrogen + H_2O	4.2×10^{15}	4200
6	Hydrogen + H_2O	2.3×10^{15}	3800
7	Hydrogen + H_2O	2.5×10^{15}	4100
8	Hydrogen + H_2O	2.9×10^{-15}	4100
9	Pure hydrogen	1.1×10^{16}	3700
10	Pure hydrogen	1.1×10^{16}	3100
11	Pure hydrogen	1.1×10^{17}	3200
12	Hydrogen + H_2O	2.3×10^{15}	4200

Consequently the Si level in solution is reduced considerably. This model has been verified by experiments in which layers were grown by turning the water vapor on and off. Under those conditions, the net donor concentration cycles in the following manner: it is high when water vapor is absent and low when water vapor is present.

Extensive Hall-effect measurements have been performed as a function of temperature on the epitaxial layers. Analysis of the data yields the donor (N_D) and acceptor (N_A) concentrations and the degree of compensation. Analysis of our data shows that in layers grown in the presence of water vapor both N_A and N_D decrease simultaneously. We believe that silicon is the only impurity in solution which is affected by water vapor. We also believe that our data indicates that silicon is an amphoteric dopant in InP.

The results of low-temperature photoluminescence (PL) evaluation of InP epitaxial layers grown in the absence and presence of water vapor in the growth ambient are shown in Figure 6. The sample grown in pure H_2 had a total carrier concentration of 8.5×10^{16} cm^{-3}. The PL spectrum obtained from this sample is dominated by broad emission bands at 1.419 eV and 1.385 eV. The 1.419 eV band is related to band edge emission and is relatively broad in this sample. The emission at 1.385 eV appears to involve donors and acceptors. In contrast, the spectrum from a sample grown in the presence of water vapor exhibits a narrower edge emission (1.419 eV) and an absence of the donor-acceptor emission. The electrical and optical evaluations discussed above show that the samples grown in the presence of water vapor are, in fact, of higher purity than the ones grown in a H ambient (with no water vapor present).

We have also performed secondary ion mass spectrometry (SIMS) studies on InP liquid epilayers grown in H ambient, as well as in samples grown in the presence of water vapor. By using Cs ions as the primary bombarding species, it has been demonstrated that the detection sensitivity for Si and other

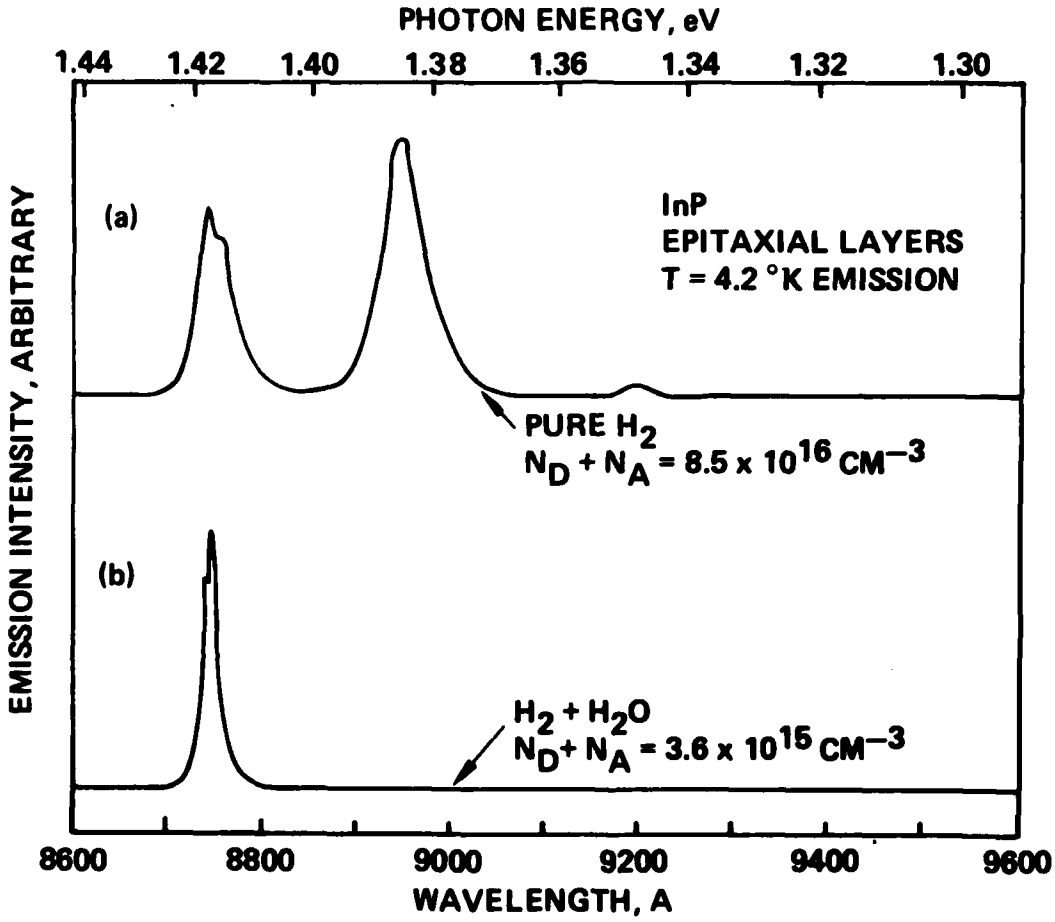

Figure 6. PL spectra of InP.

group IV elements can be improved. As seen from the data in Figure 7, it is clear that layers grown in the presence of water vapor contain smaller quantities of Si as an impurity. Similar results were also obtained from Auger electron spectroscopy (AES) studies. The chemical studies mentioned above, in conjunction with the electrical data presented earlier, clearly demonstrate that the incorporation of Si resulting from the reduction of quartz is indeed an important source of donors in LPE-grown InP.

During the course of these investigations, we observed that not all solutions responded in the same fashion (quantitatively) to the addition of water vapor. Carrier concentrations ~2 to 3 x 10^{16} cm^{-3} were measured when layers were grown from some solutions, even in the presence of water vapor in the growth ambient. These results led us to believe that an additional donor may be present in the starting solution and consequently are incorporated in the grown layers. Detailed mass spectrometry analysis of such layers reveals the presence of considerable quantities of S. The S contamination may either be associated with the starting polycrystalline material or may be caused by some other source of contamination, such as the graphite sample holder.

Since the vapor pressure of S is quite high, it is possible to reduce the S contamination by baking the growth solution at higher temperatures. Following such a bake-out, and by performing the growth at a temperature lower than the bakeout temperature in the presence of water vapor in the growth ambient, high purity InP layers can be grown, even from a contaminated solution.

During the growth experiments discussed in the earlier section, we observed severe surface degradation of InP substrates. In the growth procedure, it is essential to maintain the substrate holder (with the substrate in the hydrogen ambient) above the solution in order to ensure that they have reached thermal equilibrium with the solution. This prewarming step is necessary to prevent spontaneous nucleation around the substrate holder

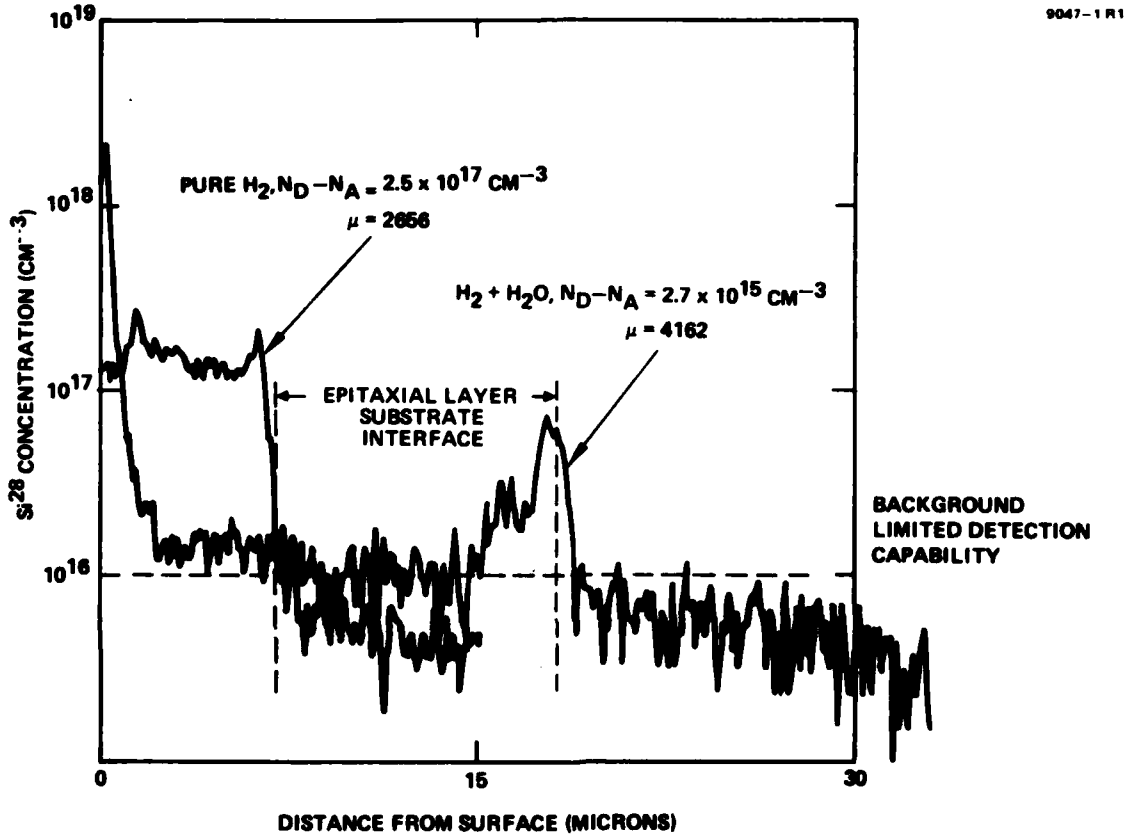

Figure 7. Secondary ion mass spectrometry (SIMS) profiles of silicon in InP layers. One layer grown in the presence of water vapor contains small quantities of Si, while another layer grown in pure hydrogen ambient contains large quantities of Si.

upon immersion into the solution. During a prewarming step, we have observed severe surface degradation of Inp substrates, primarily due to the loss of phosphorous. Such surface degradation can adversely affect the hetero-interface in the growth of InGaAs on InP. To avoid such interface problems, we have modified our sample holder, allowing us to maintain an ambient of dilute phosphine over the sample. The ability to maintain such a controlled ambient over the sample during the warming cycle will prevent any loss of phosphorus and thus reduce surface degradation.

Micrographs illustrating such surface degradation are shown in Figures 8(a) and (b). This InP sample was held above the solution in flowing hydrogen ambient at 730°C for 90 min. Thermal etch pits can be clearly seen. The pitted regions are In rich and occur due to loss of phosphorus during the high temperature process step (Figure 8(b)). For comparison, we have shown the surface features of the substrate (Figure 8(a)) prior to heat treatment. Figures 9(a) and (b) show the surface morphology of a sample subjected to the same heat treatment process in flowing phosphine ambient. Figure 9(a) shows the surface morphology of the sample prior to heat treatment, while Figure 9(b) shows the surface morphology after heat treatment. This micrograph clearly demonstrates that annealing in an ambient of flowing phosphine suppresses surface degradation. The results of these experiments show that capless annealing of InP in flowing PH_3 ambient is a viable technique for implant annealing.

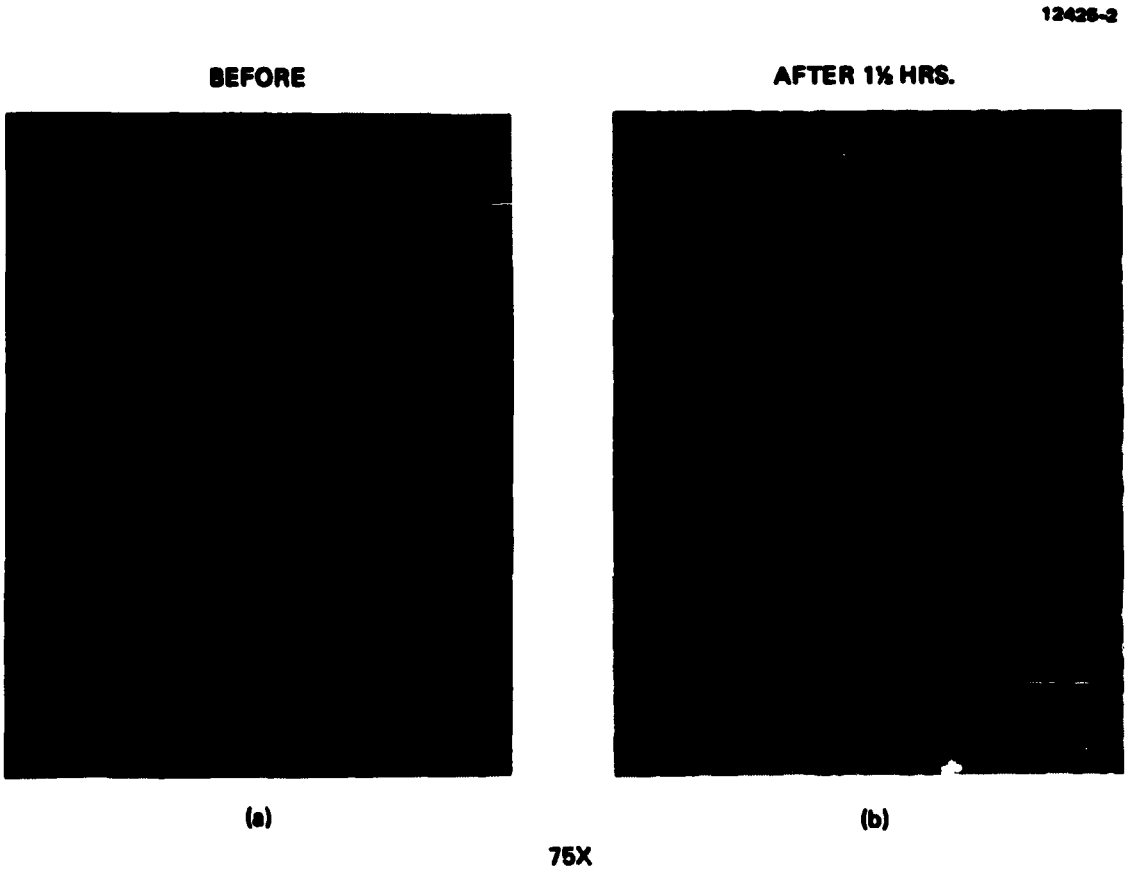

Figure 8. Decomposition of InP substrate at 730°C in H_2 ambient.

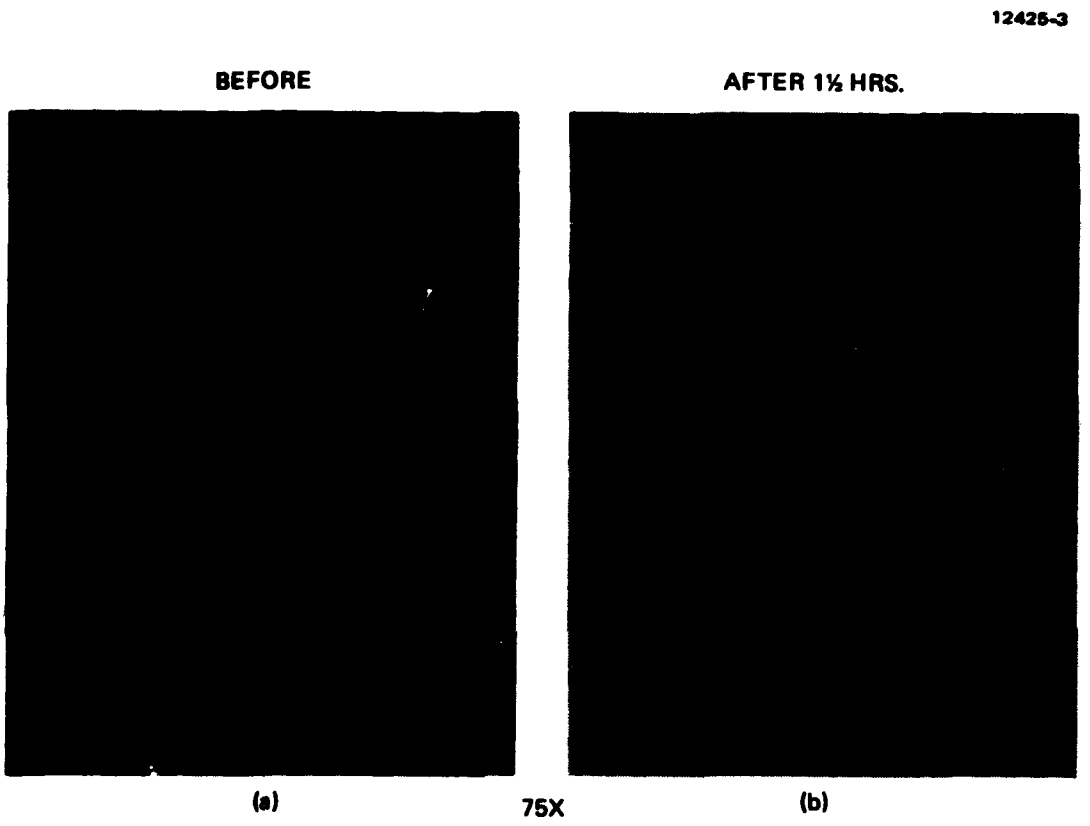

Figure 9. Decomposition of InP substrate at 730°C in H_2 ambient with PH_3.

SECTION 3

EVALUATION OF BULK InP CYRSTALS

A. INTRODUCTION

InP single-crystal ingots are normally grown by the liquid encapsulated Czochralski (LEC) growth technique using boric oxide as the encapsulant. The high vapor pressure of P over InP makes it necessary to use this growth technique.

Previous results have shown that when InP ingots are grown by the LEC technique from silica crucibles, the crystals exhibit n-type conductivity with electron concentrations in the range of low to mid 10^{16} cm^{-3}. The addition of deep level dopants such as Cr, Fe, and Co results in the growth of high resistivity InP crystals. Previous studies have shown that the doping with Fe is particularly effective and that the resultant crystals are indeed semi-insulating.

Optical and electrical measurements on Fe-doped InP samples show that Fe is a deep acceptor in InP, with an ionization energy of ~0.65 eV. The availability of semi-insulating InP makes it an attractive candidate for high speed IC applications. For such applications, it is essential that the material remain semi-insulating after high temperature processing and provide the required device isolation.

Two types of degradation can occur when InP wafers are subjected to high temperature processes. The first one occurs due to loss of phosphorus from the surface, as shown in Figure 8(b). We have also noticed this type of degradation in pulsed electron-beam-annealed InP samples. In these experiments performed in 1979 as a part of our IR&D program a highly conductive layer was present in E-beam annealed samples. Using Rutherford back-scattering analysis, workers at RADC (East) have shown that these conducting layers are formed due to loss of phosphorus from the surface. Another type of degradation is the surface conversion problem due to the redistribution of the deep level dopant during high temperature processing. This problem was encountered in

horizontal Bridgeman-grown Cr-doped semi-insulating GaAs. To achieve a quantitative understanding of this problem it is essential to develop techniques to determine the concentration of iron in InP crystals. Some of the approaches developed under this program and the preliminary results are discussed below.

Preparation of damage-free, smooth chem-mechanically polished InP surfaces is a major problem area. We have used x-ray diffraction and damage revealing etches to qualitatively evaluate the surfaces of polished InP. These details are also discussed below.

B. ESTIMATION OF Fe CONCENTRATION IN InP

In order to understand the conversion behavior observed in some Fe-doped InP crystals, it is necessary to accurately know the concentration of Fe in the starting material and to obtain the depth distribution of Fe in processed wafers.

Secondary ion mass spectrometry (SIMS) has been used to obtain the atomic concentration and the outdiffusion of Cr during implant annealing of chromium-doped horizontal Bridgeman-grown GaAs. We have used this technique to evaluate the Fe concentration in bulk InP. The analysis was performed at Charles Evans and Associates. There are severe technical problems in estimating the Fe concentration in InP. These are discussed below in detail.

In the SIMS technique, an ion beam is used to sputter the sample. The sputtered ionized atoms are then mass analyzed. In the case of iron, the dominant isotope has an atomic mass of 56. There are several combinations of molecules with mass 56. For example, a singly ionized silicon molecule (Si^+_2) has a mass of 56. Si is known to be a residual donor in InP and is present in large quantities. Interferences like this make SIMS analysis of Fe in InP somewhat uncertain. Also, in order to improve the signal-to-noise ratio, bulk analysis of the sample is performed. This type of analysis is performed at a high sputtering rate (~1.5 μm/min) using an intense primary beam. The apertures and an electrode in the ion-source in normal Cameca Instruments are

made of stainless steel. The use of intense beams can lead to sputtering from apertures and distort the analysis. During the third year of this program we will investigate the use of other chemical and physiochemical techniques to determine the iron concentration in InP.

Sample from two ingots of Inp, grown by Sumitomo Electric Corporation, and labeled A and B, were sent to Charles Evans and Associates for analysis. Both of the ingots did not exhibit any "conversion" behavior and passed our evaluation procedure described in Table 2. According to the information available from the vendor, wafers from crystal B were supposed to contain approximately 10 times the iron as compared to wafers from ingot A. Data obtained from SIMS analysis of these samples are shown in Figure 10. Within the sensitivity of the technique, it appears that both these ingots contain the same amount of iron. This apparent contradiction makes it necessary to extensively investigate this problem and use other analytical techniques to obtain the required cross correlation.

Table 2. Experimental Steps Involved in Evaluating InP Ingots

Measure resistivity of as-received sample. If $\rho > 10^7$ Ω-cm, proceed to next step.
Encapsulate the sample with ~1,500 Å PSG deposited at ~325°C.
Anneal encapsulated sample at 750°C for 30 min.
If the resistivity of annealed sample is greater than 10^6 Ω-cm, proceed to next step. If $\rho < 10^6$ Ω-cm, reject sample.
Implant silicon at 100 keV to a dose of 3×10^{12} cm^{-2}; encapsulate with PSG and anneal at 750°C for 30 min.
If the annealed sample exhibits >65% electrical activation, accept the ingot. If $\eta << 65\%$, reject ingot.

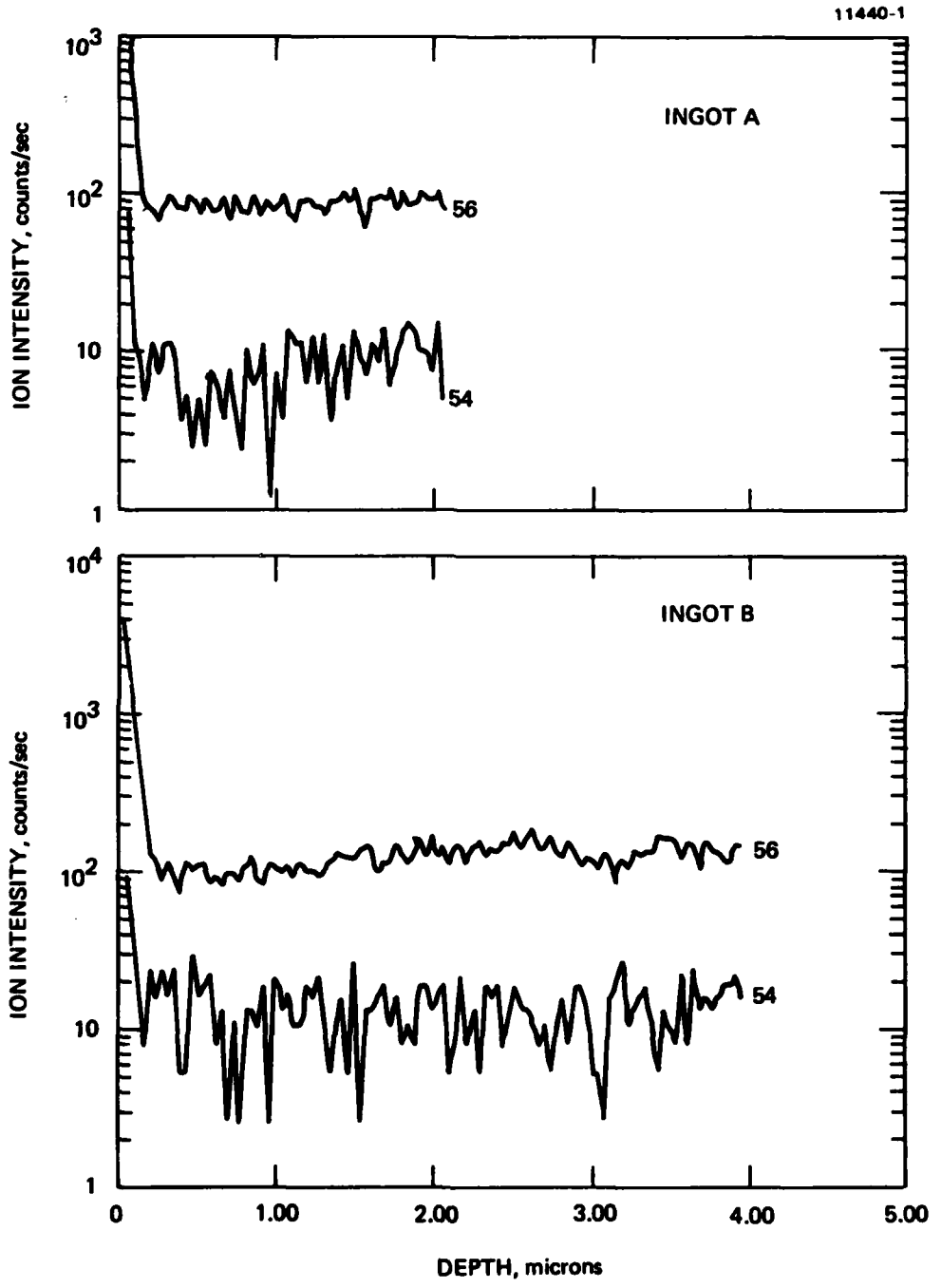

Figure 10. SIMS analysis of Fe concentration in InP ingot A and ingot B.

One chemical analysis technique is the use of Zeeman Atomic Absorption (ZAA) spectrometry. A spectrophotometer developed by Dr. T. Hadeishi of Lawrence Berkeley Laboratory has been used to analyze the chromium and manganese content in GaAs by personnel at Hughes Research Laboratories. The technique utilizes the Zeeman effect on a resonant transition and can be used to automatically correct for background interference. This correction enhances the sensitivity of the technique in comparison with that of conventional atomic absorption spectroscopy.

The element to be analyzed (for example, Fe) is introduced in a hollow cathode arc discharge lamp confined in a uniform magnetic field of about 7 to 15 kG, as shown in Figure 11. The magnetic field induces Zeeman splitting of the characteristic emission lines. The emission line at the original wavelength is called the π-line, while the split lines are called σ-lines. In addition to splitting, the magnetic field also causes the lines to be polarized; the π-line is polarized in a plane parallel to the magnetic field, while the σ-lines are polarized in a plane perpendicular to the magnetic field. Thus, by using a suitable polarizer, either a π- or σ-beam can be selected. The sample to be analyzed (in this case, InP) is introduced into an atomizing furnace to be vaporized. The π- and σ-beams are passed through these vapors and the intensity of the transmitted emission measured. The π-beam is absorbed by the sample and by light scattering and broadband molecular absorption. The σ-lines, on the other hand, are absorbed only by broadband molecular absorption and light scattering. By suitably combining the π- and σ-beams, the background contribution due to light scattering and molecular absorption can be subtracted. This unique feature of the ZAA technique increases the element detection sensitivity as well as the selectivity. Preliminary results of ZAA measurements of Fe in InP appear encouraging. The emission (or absorption) associated with Fe occurs at 248.3 nm. When a pure Fe standard is used, the absorption line is quite narrow. In contrast, the iron signals from both InP and GaAs appear to be much broader.

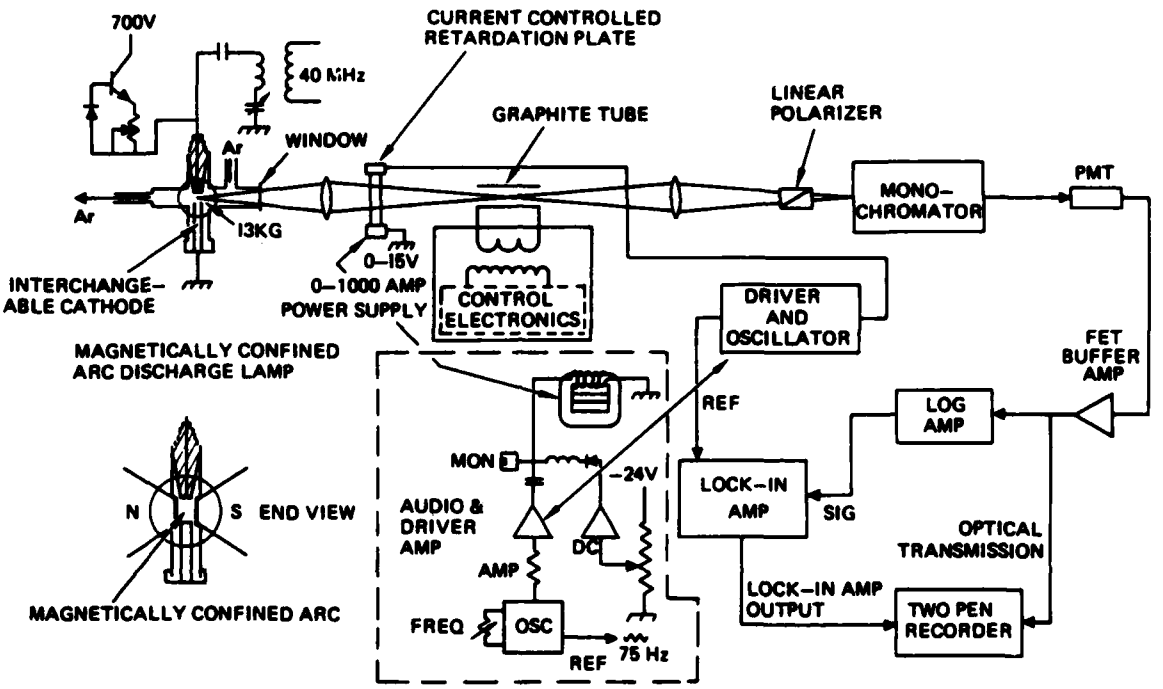

Figure 11. Schematic of Zeeman atomic absorption spectrometer.

Detailed and quantitative studies of Fe in InP will be undertaken in our 1982 program. We will also perform cooperative measurements with workers at Air Force Avionics Labs (Spark Source Mass Spectrometry) in 1982 to address the problem of quantitative measurement of Fe content in InP.

We have performed SIMS measurements on wafers from ingots A and B which were encapsulated with PSG (phosphosilicate glass) and annealed at 750°C for 30 min. The Fe distribution in annealed samples did not differ significantly from the unannealed control samples. These samples passed our qualification test described in Table 2. However, in ion implanted samples subjected to 700°C anneal, dramatic depletion of iron in the near surface region, along with a pile up at the surface, was observed. These results are discussed in the next section on ion implantation studies. While quantitative determination of Fe concentration is in question, the qualitative redistribution of Fe in ion-implanted InP is clear. More detailed studies will be performed in our 1982 program.

C. SURFACE PREPARATION OF InP

In most FET devices the conduction between the source and drain takes place in the near surface region. The presence of surface damage can reduce the surface carrier mobility, thus degrading device performance. Such degradation can be minimized by preparing damage-free, smooth surfaces by appropriate procedures.

In this study we have concentrated on evaluating the surface perfection of InP samples by using chemical etching (to reveal subsurface damage) and by x-ray techniques. Material as received from two vendors was evaluated. The surface of the material from vendor A appeared specular mirror-like, and featurelss. While the surface of material from vendor B appeared to exhibit an orange-peel-like appearance. On etching the surface of wafers from vendor A in a 5% solution of bromine in methanol, extensive

surface pitting, indicative of the presence of surface damage in InP, was observed. Wafers from vendor B did not exhibit such surface features on etching. The micrograph in Figure 12 illustrates the presence of surface damage in samples obtained from vendor A.

We have also evaluated the InP wafers by performing x-ray diffractometer studies using the double refractometer arrangement. CuK_{α} lines were used. The samples from vendor A exhibit extensive line broadening, while those from vendor B exhibit sharp featured lines. The line widths from sample B are normal and are instrument limited (as shown in Figure 13). Later, it was learned that the samples from vendor A were polished in a slurry of 0.05 μm zironium oxide, while vendor B used chem-mechanical polishing in a 5% solution of bromine in methanol as the last polishing procedure. These studies show that the chem-mechanically prepared surfaces can be damage free but are not, unfortunately, mirror-like and smooth. We have used x-ray diffraction and selective area electron diffraction (psuedo-kikuchi) techniques to ensure the crystallinity of the wafers.

Figure 12. Micrograph showing extensive surface damage revealed by etching mechanically polished InP from Vendor A in a solution of 2% Br in methanol for 1 min.

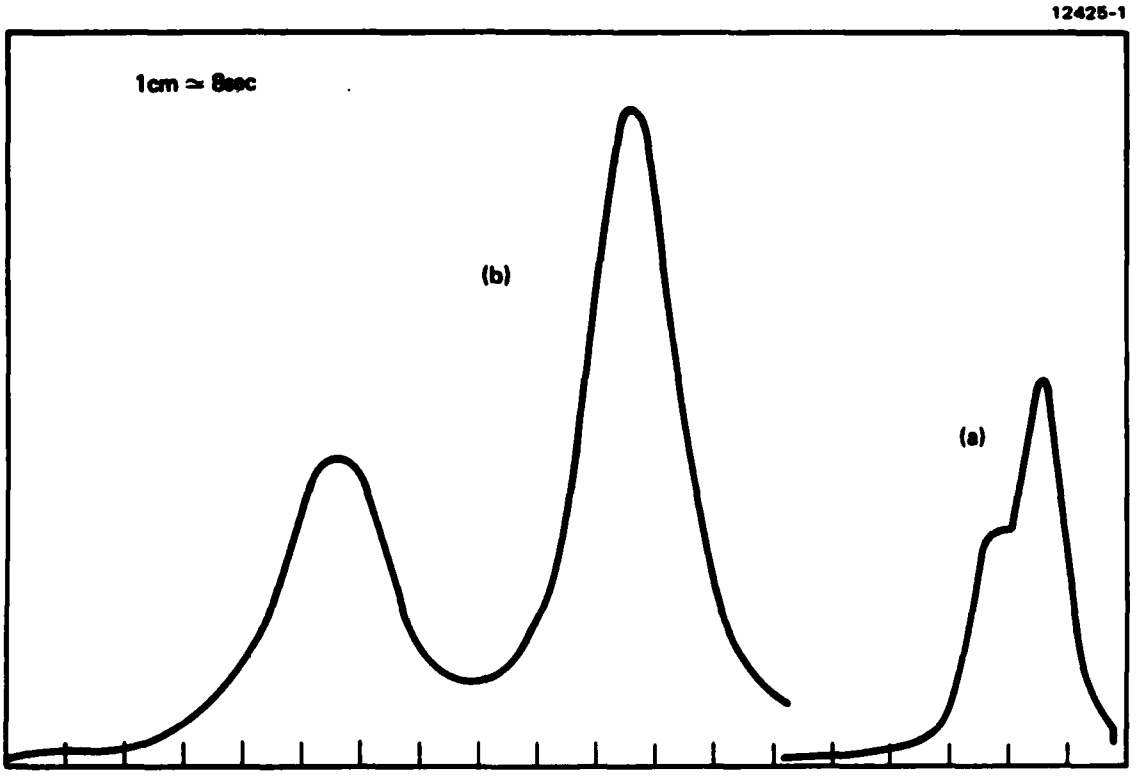

Figure 13. X-ray (rocking curve) data obtained from two InP samples. (a) Chemically polished. (b) Mechanically polished.

SECTION 4

ION IMPLANTATION DOPING STUDIES

A. INTRODUCTION

Ion implantation is a versatile method of doping semiconductors. The dopant concentration and depth of the doped regions can be independently controlled by varying the implantation dose and energy appropriately. The ion implantation process damages the crystal lattice; thus it is necessary to anneal the damage by appropriate heat treatment. This heat treatment supplies the necessary thermal energy that is imparted to the crystal to ensure that the active dopants are located at the appropriate locations in the lattice to be eletrically active.

High temperature annealing of InP is complicated by the excessively high phosphorus vapor pressure over the sample at the anneal temperature. It is, therefore, necessary to encapsulate the sample with an appropriate encapsulant or perform the anneals in a carefully controlled ambient. During the course of these AFOSR-sponsored studies, we have investigated the effectiveness of SiO_2, Si_3N_4, phosphsilicate glass (PSG) and a combination of a thin Si_3N_4 overcoated with PSG as annealing encapsulants. Some of the results from such studies have been reported in an earlier report, but will be repeated here for the sake of completeness.

B. ANNEALING STUDIES

Hughes Research Laboratories (HRL) has developed several systems capable of depositing a variety of dielectrics for application to compound semiconductor device fabrication as part of our extensive IR&D program. Silicon dioxide and phosphosilicate glass are deposited by a pyrolytic process and silicon nitride by a plasma enhanced deposition process. The results of investigations to evaluate the integrity of these layers following high temperatures annealing are discussed below. SiO_2 films were deposited by a pyrolytic process at 330°C in a cold-wall system operating at atmospheric pressure. The samples were placed on a

graphite susceptor which was heated inductively by an rf coil surrounding the reaction chamber. An electronically controlled ramping system ensured that the samples could be brought from 280°C to the deposition temperature (up to a maximum of 750°C) in a few seconds. Typical gas flow rates used for SiO_2 deposition are:

Nitrogen	42 l/min
SiH_4	11 cm^3/min
Oxygen	210 cm^3/min

The nitrogen flow ensures that the reactor is flushed during deposition and does not enter into the reaction. PSG layers with ~8 atomic percent phosphorus in SiO_2 could be deposited at 330°C by adding 1.9 cm^3/min of PH_3. The PSG films exhibited an index of refraction (EADAX) and Auger Electron Spectroscopy (AES) confirmed that the phosphorus content in these layers was approximately 8%. The silicon nitride layers were deposited by a plasma enhanced deposition process, with the substrates held at ~250°C.

The surface morphology of an InP sample annealed at 700°C for 30 min with SiO_2 encapsulant in the flowing forming gas ambient was examined in a Cambridge 150 stereoscan scanning electron microscope. Examination with the SiO_2 in place revealed the presence of cracks in the encapsulants. On removal of the SiO_2 layer, shiny tracks on the surface of InP were observed. These are shown in Figure 14. A magnified view of such shiny tracks is presented in Figure 15 and clearly shows extensive surface damage. A X-ray dot map of the same region in Figure 15 from EDAX analysis of the sample is illustrated in Figure 16. The EDAX data is in close agreement to that shown in Figure 15. From this data we conclude that in the regions where the encapsulant

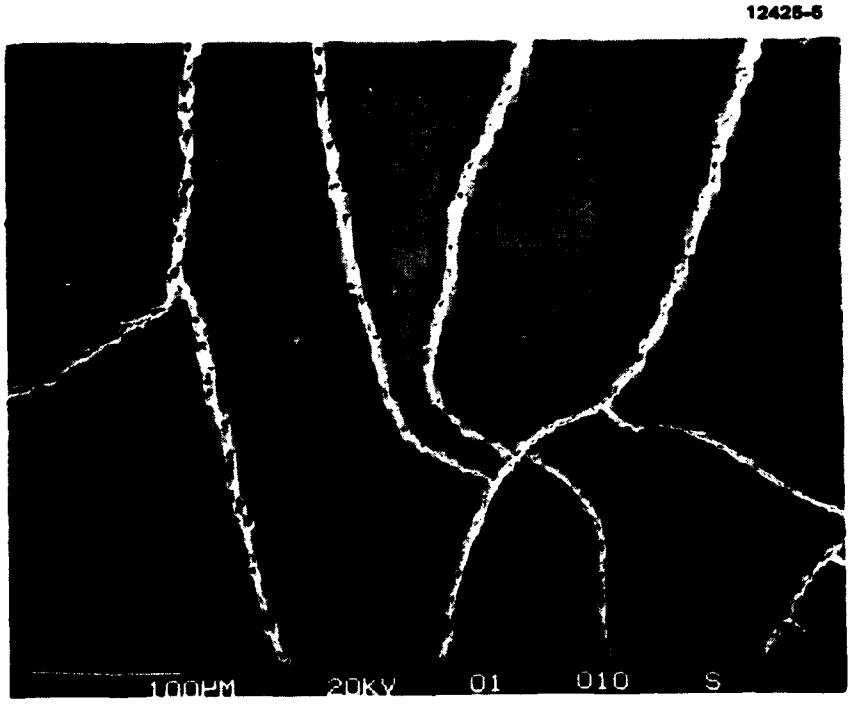

Figure 14. SEM micrograph of an InP sample annealed with SiO_2 encapsulant at 700°C for 30 min. The shiny regions in this micrograph are In rich regions.

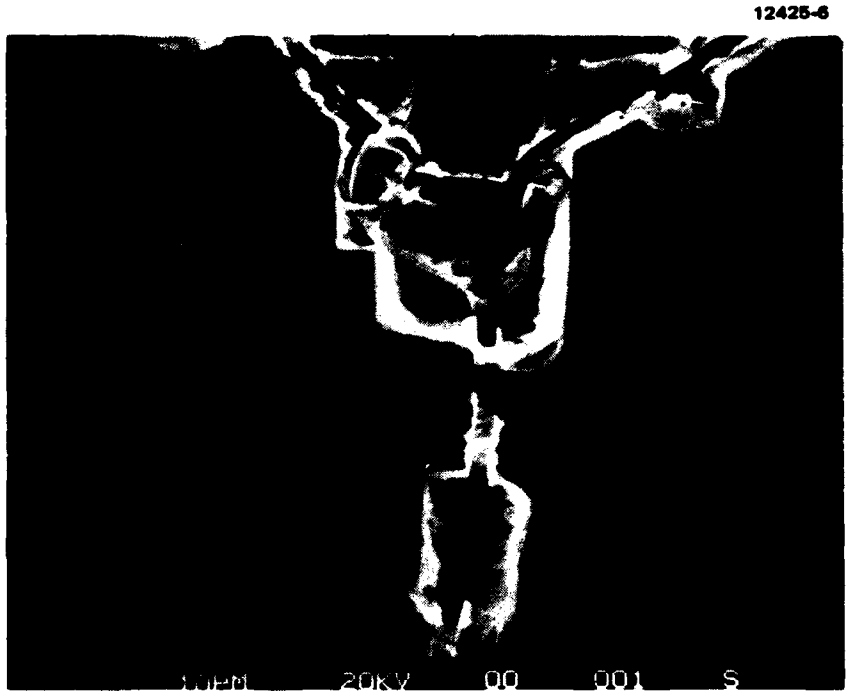

Figure 15. A magnified view of an In rich region from the sample shown in Figure 14.

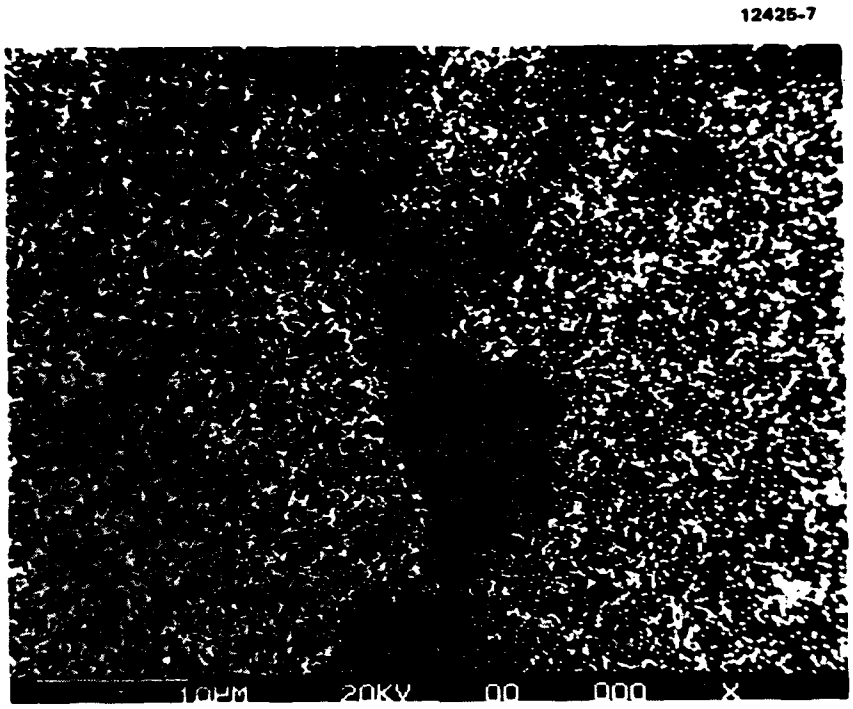

Figure 16. X-ray dot elemental image of region in Figure 15. The figure shows the distribution of indium.

ruptured during the high temperature annealing process, a considerable loss of phosphorus ocurred in regions where the molten excess indium solidified (light regions in the micrographs). In the case of samples annealed with phosphosilicate glass (PSG with ~8% P in SiO_2) encapsulant, the presence of such surface degradation was considerably less.

In the case of samples annealed with a thin layer (~400 Å) of Si_3N_4 overcoated with ~1000 Å PSG layers, little or no surface degradation was observed on annealing at 700°C for 30 min. This anneal process is the base line approach in our InP-based IC program.

These studies clearly demonstrate that the use of PSG as an anneal cap is effective in performing the implantation activation annealing process. The results discussed in Section 2 (Figure 9) show that capless annealing in flowing PH_3 ambient is effective in reducing surface degradation. We will evaluate the effectiveness of annealing ion-implanted InP samples in flowing PH_3 ambient in detail in our 1982-83 program with our dedicated capless annealing furnace.

C. ELECTRICAL EVALUATION OF ION IMPLANTED LAYERS

Hall effect measurements were performed on ion implanted and annealed InP samples. The process parameter studied included various dopant ions, implant temperature, energy, fluence, anneal temperature and the use of different encapsulants during anneal. Both p-type (Be and n-type dopants (C, Si, Si, Sn, and Se) were studied. The details of such studies are described in this section. The results show that it is easier to achieve high doping levels and percentage activation with donor dopants. Secondary ion mass spectrometry (SIMS) shows that little or no redistribution effects occur following high temperature annealing with n-type dopants, even at high concentrations. Dramatic redistribution occurs in Be-implanted samples at high concentrations, even at anneal temperatures as low as ~650°C.

Preliminary SIMS studies show the redistribution of Fe in ion-implanted and annealed InP samples. The redistribution of Fe in implanted InP is qualitatively similar to the redistribution of chromium in horizontal Bridgeman-grown semi-insuating GaAs. More detailed measurements are necessary to quantitatively understand the behavior of Fe in InP.

1. Be-Implanted InP

Beryllium is known to be a shallow acceptor in several III-V compound semiconductors. It has an atomic mass of 9 and causes little damage to the lattice. Extensive optical studies in GaAs have shown that the lattice damage introduced by Be anneal out at ~400°C, and that almost complete electrical activation can be accomplished at an anneal temperature as low as 500°C.

The measured sheet hole concentration and the hole mobility are plotted in Figure 17 as a function of anneal temperature from InP samples implanted with 300 keV Be^+ to the fluences indicated. At low doses, the measured sheet hole concentration increases monotonically with anneal temperatures. Over 80% of the implanted Be becomes electronically active following an anneal at 750°C for 30 min. In the case of high dose (1×10^{14} cm^{-2}) implanted samples, the maximum percentage activation (~65%) was measured in samples annealed at ~700°C. The measured sheet carrier concentration decreased slightly on annealing at 750°C. There was a slight but gradual increase in hole mobility with increased anneal temperature.

In order to establish a threshold anneal temperature for electrically activating Be in InP, samples were implanted with 100 keV Be to fluences ranging from 1×10^{13} cm^{-2} to 1×10^{14} cm^{-2}. All the samples were encapsulated at 330°C with phosphosilicate glass and were subjected to higher temperature anneals for 30 min in an ambient of flowing, forming gas. The lowest anneal temperature used in this study was 330°C (same as PSG deposition temperature). Following the anneal and removal of PSG, ohmic contacts were formed and the samples were electrically

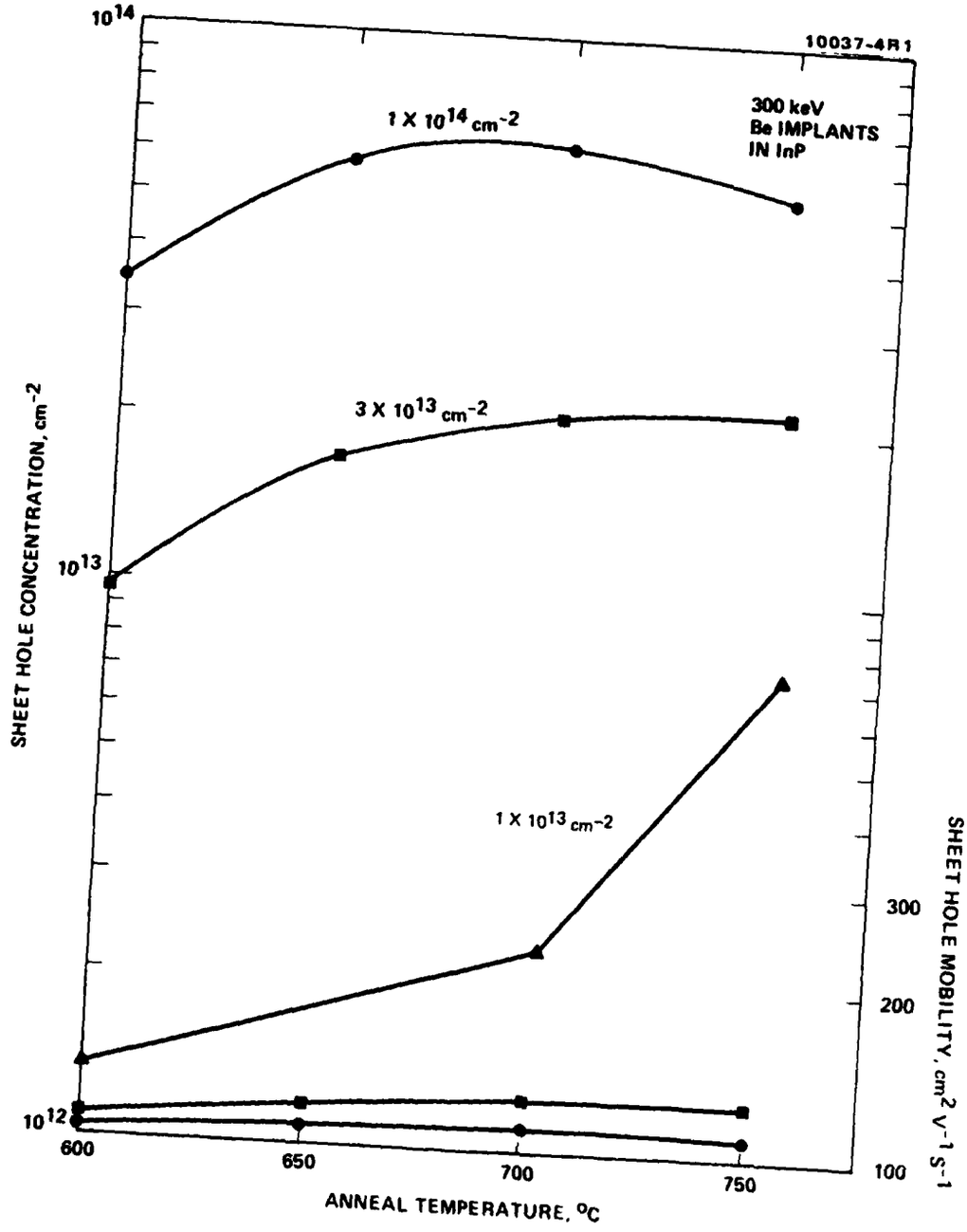

Figure 17. Measured sheet hole concentration and hole mobility as a function of anneal temperature from InP samples implanted with beryllium to fluences shown.

evaluated. Figure 18 shows the variation of measured carrier concentration as a function of anneal tmeperature for the Be-implanted samples. For anneal temperatures between 330°C and 400°C, the samples remained high resistivity n-type (carrier concentrations ~10^8 el/cm^2). It apears that implantation-induced defects in InP are donor-like centers. However, at anneal temperatures between 500°C and 550°C the layers became strongly p-type, with a large fraction of the implanted dopants becoming electrically active. This sharp annealing threshold is similar to the annealing behavior of Be-implanted GaAs. We will perform optical studies of low temperature (550°C) annealed InP in collaboration with Prof. W.G. Spitzer and co-workers at the University of Southern California. These studies will be carried out as a part of our IR&D program.

We have used SIMS to obtain the atomic distribution of Be from as-implanted and annealed samples. Figure 19 shows the as-implanted distribution of Be-implanted to a dose of 3 x 10^{13} cm^{-2} at energies of 150 keV, 300 keV, and 600 keV. The depth scale (x-axis) was calibrated by measuring the depth of the SIMs craters with a Sloan Dektak system. The atomic concentration (y-axis) can be calibrated by assuming that the integrated Be atom concentration within the Gaussian is equal to the implant fluence. The peak of the distribution occurs at nearly the projected range, as calculated by LSS theory. The shape of the dopant profile is not symmetrical and appears to be skewed to the surface. With a light projectile like Be thrust in a target composed of heavy elements like InP, such skewing towards the surface is expected. Such non-symmetrical profiles can be described by a modified Pearson IV distribution.

In the case of low fluence implants (1 x 10^{13} cm^{-2}, 300 keV) annealed (700°C, 30 min with PSG encapsulant) Be profiles do not differ significantly from the as-implanted profile. In the case of samples implanted to a fluence of 1 x 10^{14} cm^{-2}, dramatic redistribution effects can be observed, even in samples annealed at 650°C for 30 min. The as-implanted and annealed (650°C and

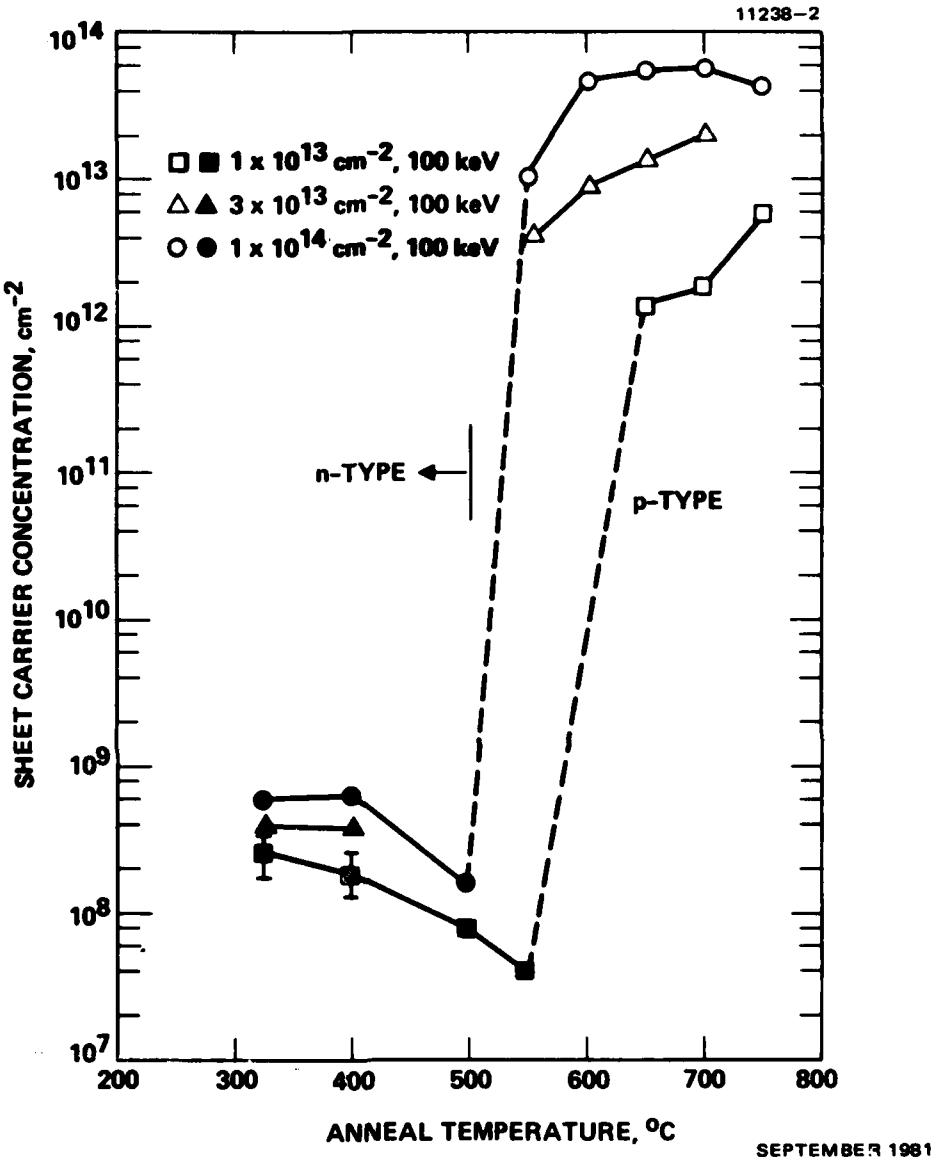

Figure 18. Measured sheet carrier concentration as a function of anneal temperature from Be-implanted InP samples.

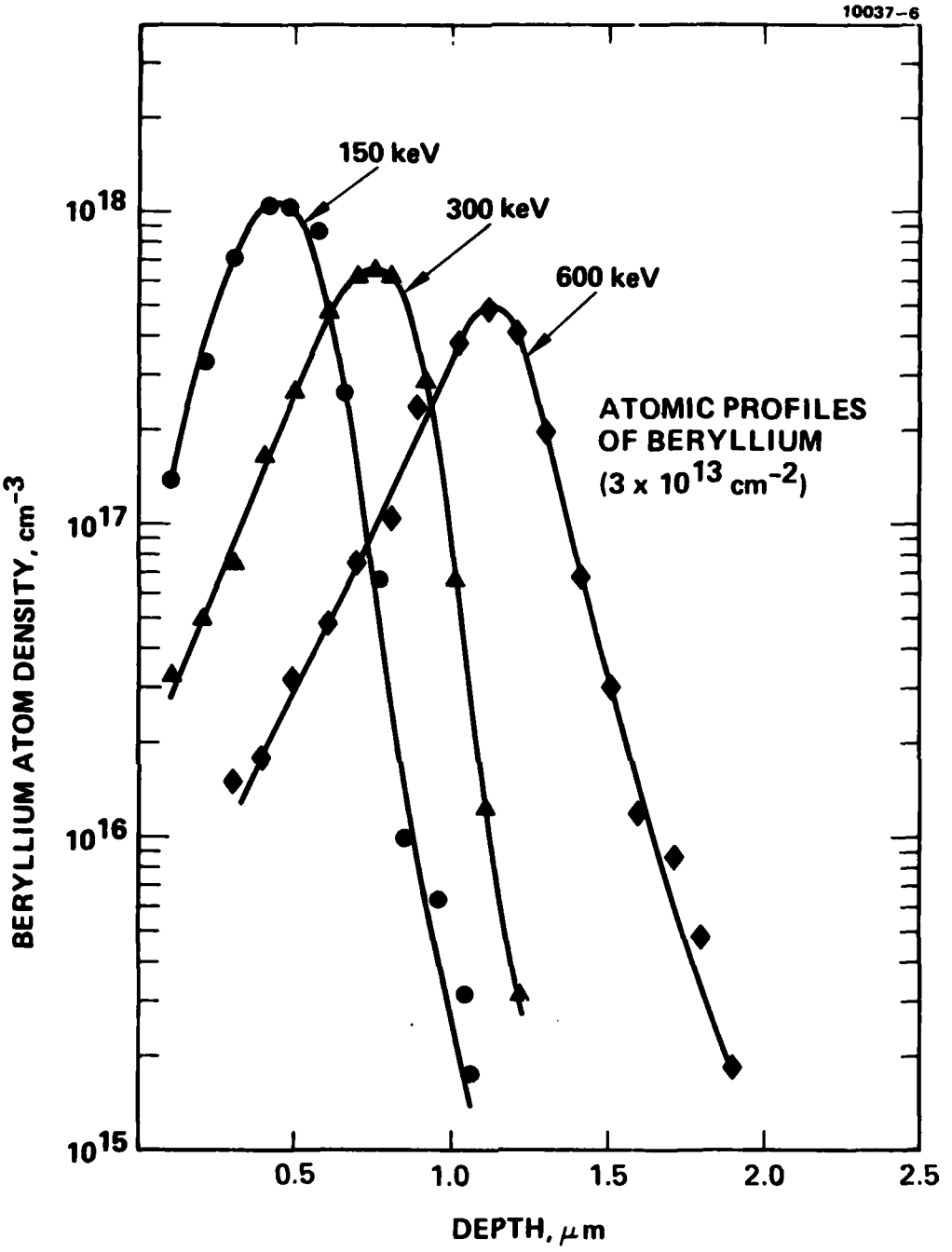

Figure 19. Atomic distribution of ion-implanted Be in InP. The implant energies were 150 keV, 300 keV and 600 keV with an implant fluence of 3 x 10^{13} cm-2.

700°C anneals) Be profiles obtained from InP samples are shown in Figure 20. The results are qualitatively similar to the annealing behavior of high fluence Be-implanted GaAs, except that some features in the redistributed profiles are different. A more detailed and thorough study of such redistribution effects needs to be performed to understand this effect.

2. Electrical Evaluation of n-Type Dopants

Among all potential n-type dopants in InP, carbon has the lightest atomic mass. It is only slightly more massive than Be, and the damage introduced by C is not expected to be very different from that due to Be. Since Be can be activated at an anneal temperature as low as 550°C (as shown in the previous section), we decided to investigate the annealing behavior of carbon-implanted InP.

Samples were implanted with 200 keV C at doses ranging from 1×10^{13} cm^{-2} to 2×10^{14} cm^{-2}. These samples were encapsulated with PSG and annealed at temperatures ranging from 550°C to 750°C. Electrical measurements reveal that only ~3% of the implanted dopants became donor-like, even when annealed at 700°C. In fact, even after annealing at 750°C for 30 min, <5% of the implanted C became electrically active. Electron mobilities measured in 750°C – annealed, low fluence (1×10^{13} cm^{-2}), implanted samples were only 2000 $cm^2 V^{-1}s^{-1}$. The low electrical activation and low measured carrier mobilities encountered in C-implanted InP leads us to speculate that carbon acts as an amphoteric dopant in InP. Low temperature photoluminescence and local mode vibrational spectroscopic measurements and annealed InP samples may provide some answers to this paradox. Another explanation may be that most of the carbon atoms on annealing occupy interstitial sites. Regardless of the mechanism involved, carbon does not appear to be an efficient n-type dopant in InP.

Silicon, which is a group IV element, is a potential dopant in InP. Although silicon is an amphoteric dopant in III-V

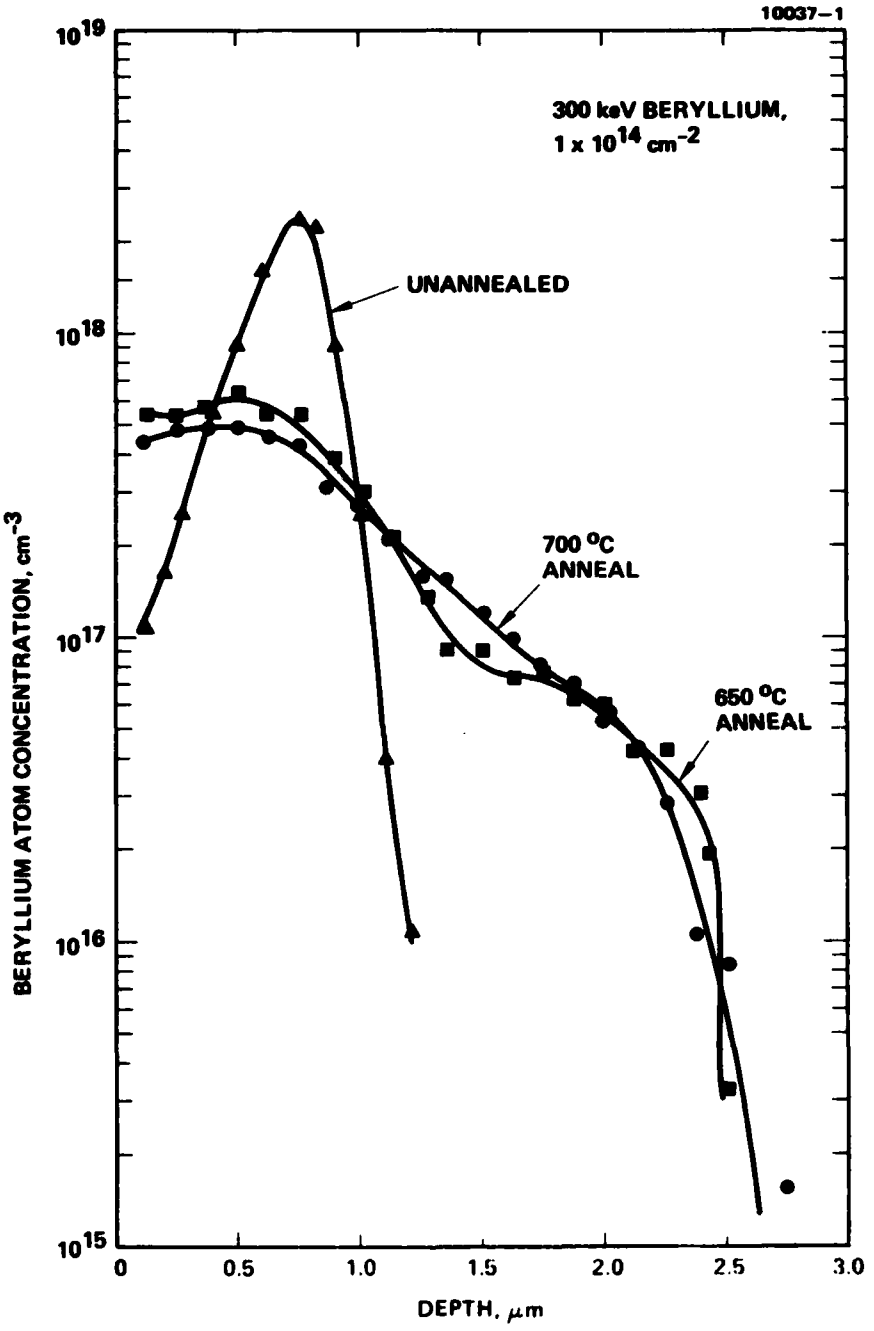

Figure 20. Atomic distribution of ion-implanted Be obtained from unannealed and annealed InP samples showing effects of drastic redistribution.

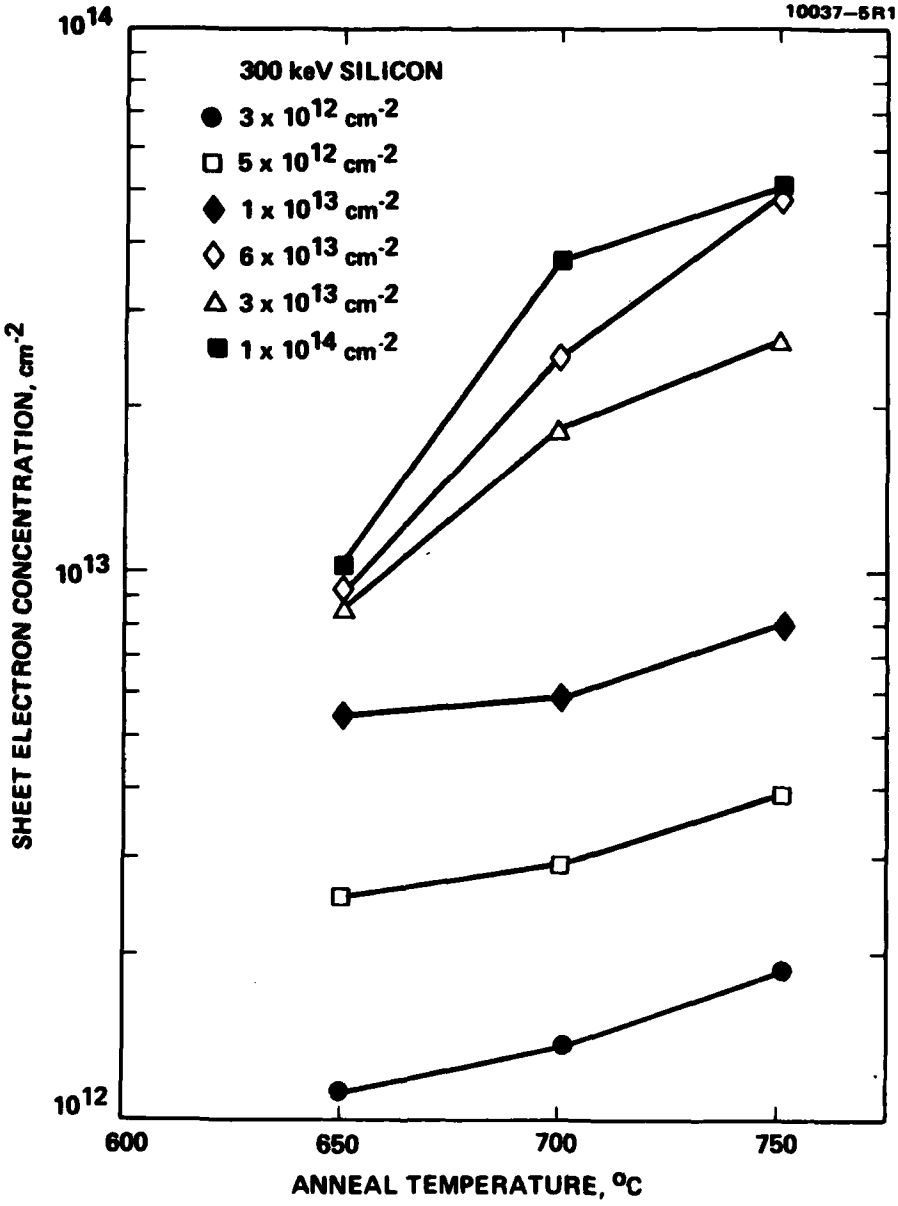

Figure 21. Sheet electron concentration as a function of anneal temperature in InP samples implanted with silicon ions to fluences indicated.

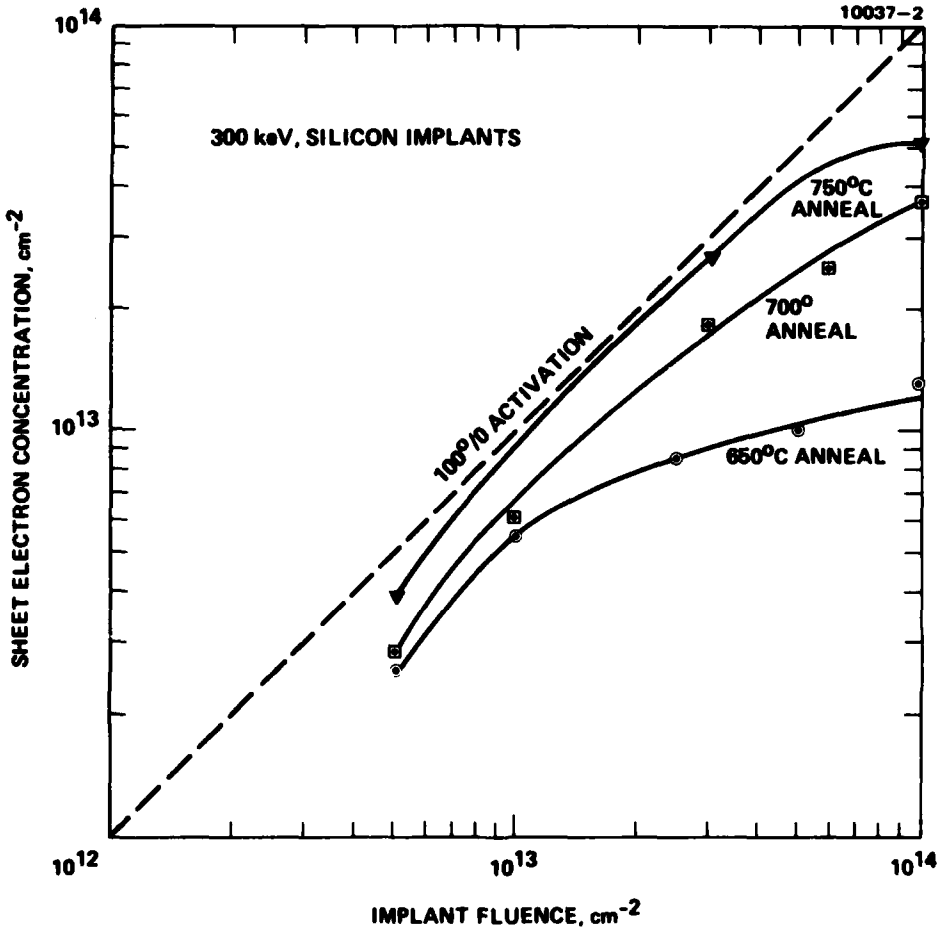

Figure 22. Sheet electron concentration as a function of implant fluence of 300 keV Si-implanted InP samples.

semiconductors, silicon introduced by ion implantation acts primarily as a donor in GaAs. The present studies clealy show that a similar trend holds good in InP and that silicon is a well-behaved donor dopant in InP.

A wide range of implantation and anneal parameters were covered in this study, including implant doses from 3×10^{12} cm^{-2} to 1×10^{14} cm^{-2}, with an implant energy of 300 keV. Some implants were also performed at 100 and 600 keV. The samples were annealed over a temperature range from 650°C to 750°C. Most of the studies described in this section were performed using PSG as the annealing encapsulant. Results obtained from samples annealed with a thin Si_3N_4 (~400 Å) and overcoated with PSG were essentially indistinguishable from samples annealed with a PSG encapsulant alone.

In Figure 21, we show the variation of measured sheet electron concentration (cm^{-2}) and the sheet electronmobility (cm^2 $V^{-1}s^{-1}$) for InP samples implanted to fluences shown as a function of anneal temperature. In the anneal temperature range covered in this study, the measured carrier concentration increased monotonically with the anneal temperature.

As seen in Figure 21, in the case of low fluence implanted samples ($<3 \times 10^{12}$ cm^{-2}), over 80% of implanted atoms became electrically active on annealing at ~750°C for 30 min. Carrier mobilities as high as 2900 cm^2 $V^{-1}s^{-1}$ were measured in 5×10^{12} cm^{-2}-implanted samples annealed at 750°C. In the case of high fluence implanted samples ($>6 \times 10^{13}$ cm^{-2}), the measured sheet electron concentration appeared to saturate at ~5×10^{13} cm^{-3} following an anneal at 750°C for 30 min. At such concentrations, typical mobilities of 1500 cm^2 $V^{-1}s^{-1}$ were measured.

It is more informative to plot the measured carrier concentration as a function of implantation fluence for various anneal temperatures. Such nformation is summarized in Figure 22. The complete (or 100%) activation line is shown by the dotted line in this figure. The three solid curves represent the data obtained from samples which were annealed at 650, 700, and 750°C,

respectively. As seen from this figure, it is clear that for samples implanted to fluences ranging from 8 x 10^{12} cm^{-2} to 4 x 10^{13} cm^{-2}, over 90% electrical activation can be achieved following an anneal at 750°C. The data shown for silicon represents the average data from a large number of InP samples and represents the baseline implant data for forming the source-drain regions for our MISFET IC program.

We have also evaluated the as-implanted and annealed (700°C, 30 min with PSG encapsulant) profiles of silicon-implanted at InP. The data, shown in Figure 23, show little or no difference between the as-implanted and annealed profiles, even at high silicon atom concentrations. This data clearly indicates that in contrast to the behavior of Be (acceptor)-implanted InP, silicon implanted InP exhibits little or no redistribution behavior in InP even at concentrations in excess of 1 x 10^{18} cm^{-3}.

Germanium is known to be an amphoteric dopant in III-V compound semiconductors. Depending upon the implantation (implant fluence and temperature) and process parameters (annealing temperature, encapsulant used) implanted Ge can either can act as donors or acceptors in GaAs. We have investigated the annealing behavior of InP samples implanted with Ge. For the conditions covered in this study, all Ge-doped layers exhibited strong n-type conductivity with a high degree of carrier activation.

Several InP samples were implanted with Ge to fluences ranging from 6 x 10^{12} cm^{-2} to 3 x 10^{11} cm^{-2}, with implant energies of either 150 keV, 300 keV, or 600 keV. The samples were encapsulated with either PSG or Si_3N_4 and were annealed at temperatures ranging from 650°C to 750°C for 30 min.

The variation of measured sheet electron concentration and sheet electron mobility are shown as an implant fluence in Figure 24 for anneal temperatures of 650, 700, and 750°C. All these data were obtained from samples implanted with 600-keV Ge ions. The complete (100%) activation curve is also shown (by the

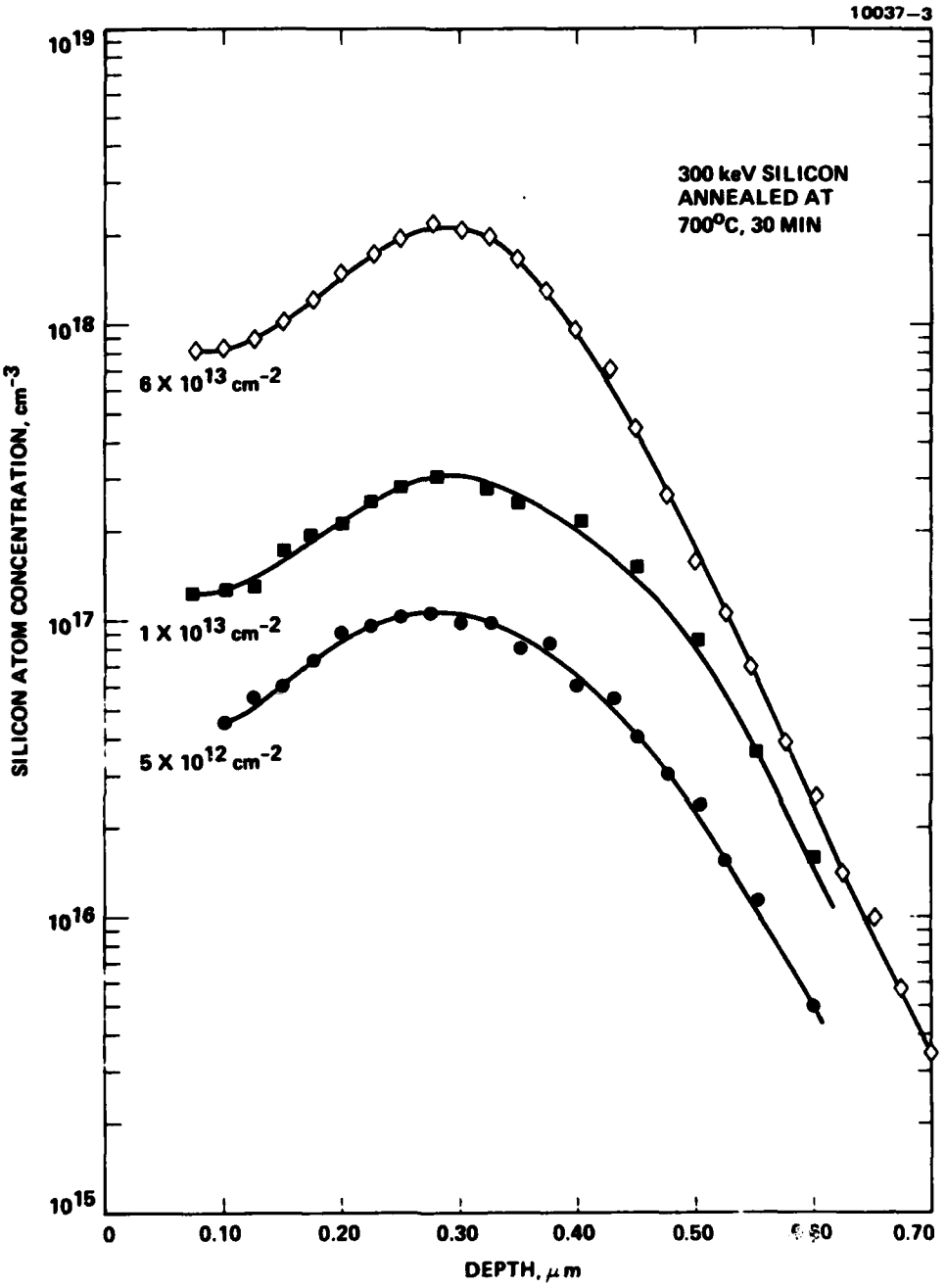

Figure 23. Atomic distribution obtained from Si implanted and annealed InP samples.

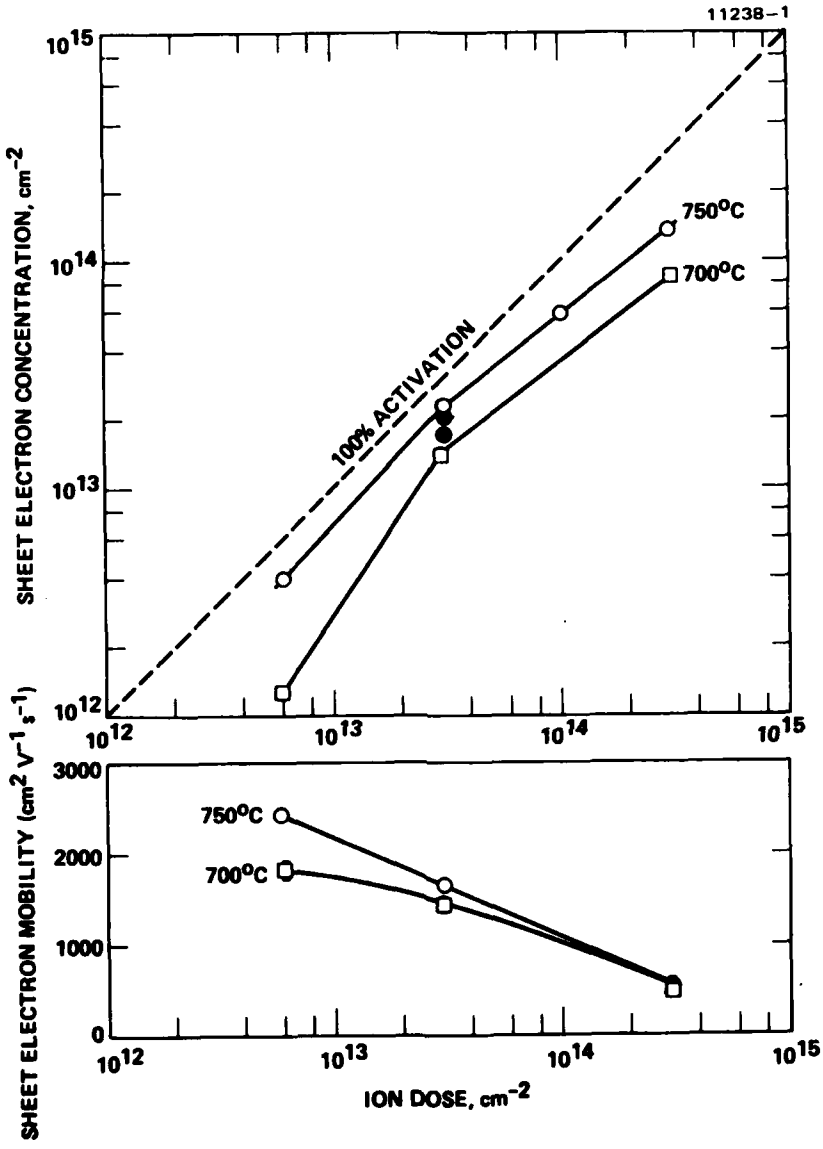

Figure 24. Sheet electron concentration and sheet electron mobility in Ge-implanted InP samples as a function of implantation dose and annealed at 700°C and 750°C.

dashed line) in this figure. For the intermediate dose range (from 6 x 10^{12} cm^{-2} to 5 x 10^{13} cm^{-2}), high carrier activation is achieved on annealing at 750°C. For much higher doses, the activation decreases to ~40% or 80%. The measured mobilities in 750°C-annealed samples range from ~2200 cm^{-2} $V^{-1}s^{-1}$ to ~650 cm^2 $V^{-1}s^{-1}$. We also observed that higher activation with high carrier mobilities were achieved in samples with higher energy ions. For example, in samples implanted with 600 keV, 3 x 10^{13} cm^{-2} Ge ions and annealed at 750°C sheet carrier concentrations of 2.3 x 10^{13} cm^{-2} and mobilities of 1280 cm^2 $V^{-1}s^{-1}$ were measured while the same fluence at 150 keV and annealed at 750°C exhibited sheet carrier concentrations of 1.9 x 10^{13} cm^{-2} with cm^{-2}, with carrier mobilities of 730 $cm^2V^{-1}s^{-1}$. These data indicate that the residual defects in the near surface region play a major role in carrier transport properties of Ge-implanted InP. We also observed that consistently higher carrier activation and mobilities can be achieved in samples annealed with PSG encapsulant. Preliminary data indicates that high fluence of implants at 150°C show higher carrier activation and higher carrier mobilities than room temperature implants. A more detailed study of hot implants will be the focus of our 1982 program.

The distribution of Ge atoms, as obtained by SIMS measurements, from as-implanted and annealed (780°C) InP samples are shown in Figure 25. The experimental data show that little or no redistribution of implanted Ge takes place on annealing, even at high concentrations. These results are in agreement with data from Si-implanted samples, but are in complete contrast to the atomic redistribution observed in Be-implanted and annealed samples. Drastic diffusional broadening of other acceptor-implanted dopants (Zn, Cd, Mg) are known to occur in InP and other III-V compound semiconductors. During 1982 we will use our experimental data to develop theoretical models which can explain the diffusion behavior of donor and acceptor dopants in these materials.

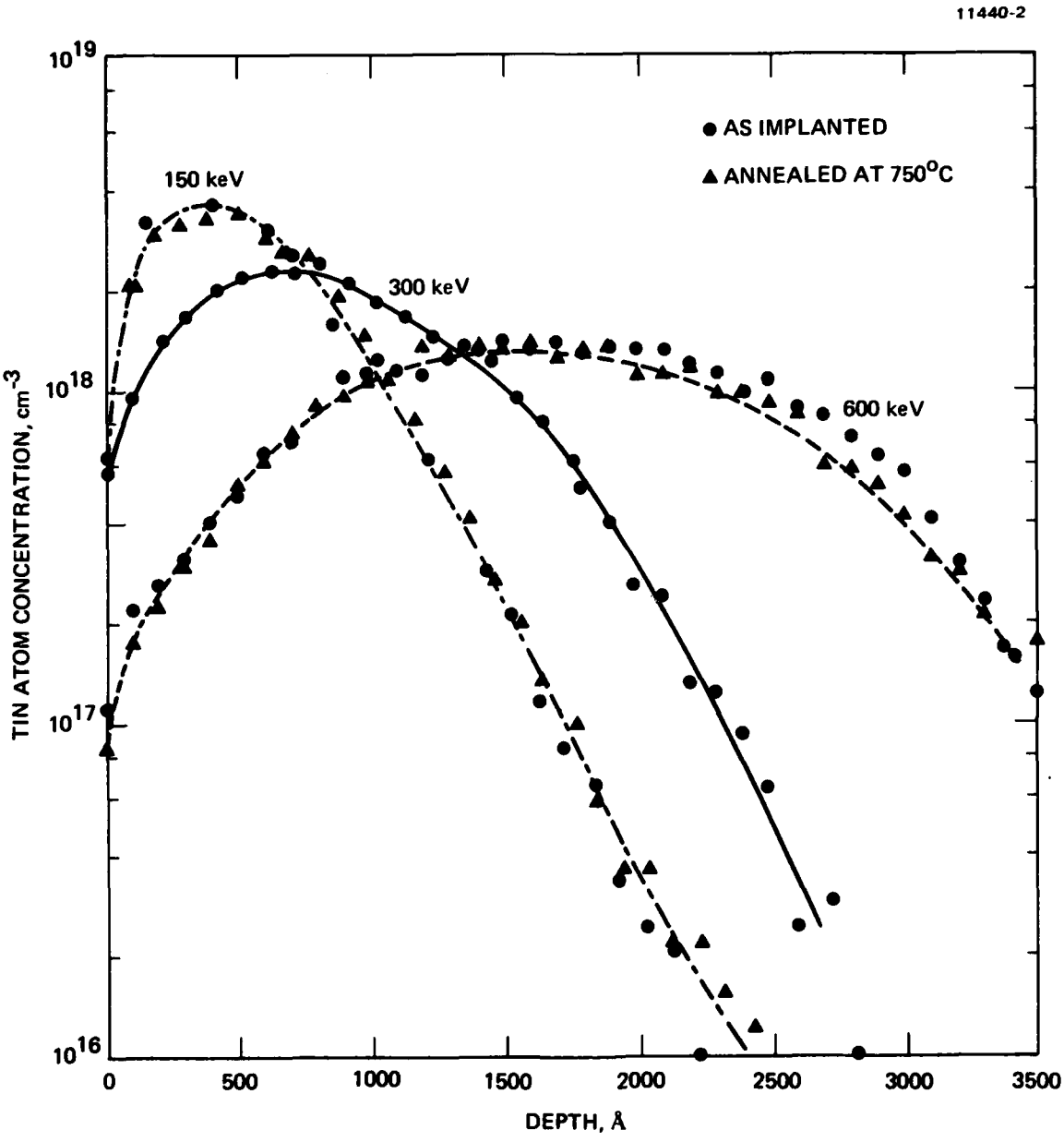

Figure 25. SIMS atomic distributions of Ge obtained from As-implanted and annealed InP samples.

Preliminary experiments on Sn-doped InP layers indicate that Sn is a well-behavied donor dopant in InP. Table 3 describes the results obtained from 150 keV, 300 keV, or 600 keV Sn^+ implants (3×10^{13} cm^{-2}). The data clearly demonstrate that high activation can be achieved in samples implanted with Sn at elevated temperatures. These experimental results show that recrystallization of heavily damaged or amorphorized compound semiconductors is a major problem. To understand the recrystallization mechanism involved, we will perform time resolved reflectivity (TRR) and Rutherford backscattering (RBS) measurements on heavily damaged and annealed InP samples.

We have also investigated the annealing behavior of Se-implanted InP. In Figure 26, we show the variation of measured sheet electron concentration and sheet mobility as a function of implantation dose for two anneal temperatures. As seen from this data the anneal behavior of Se in InP is the same as those of Si, Ge, and Sn-implanted samples. Samples have been implanted with Se at ~150°C for various fluences and will be evaluated during 1982.

Table 3. Electrical Properties of Sn-Implanted InP
Implant Fluence: 3×10^{13} cm^{-2}

Energy, keV	Anneal Temperature, °C	Sheet Electron Concentration, cm^{-2}	Sheet Electron Mobility, $cm^2\ V^{-1}s^{-1}$
150	700	$(1.08 \pm 0.05) \times 10^{13}$	1200 ± 10
300		$(1.72 \pm 0.05) \times 10^{13}$	1310 ± 40
600		1.73×10^{13}	1531 ± 52
150	725	$(1.86 \pm 0.15) \times 10^{13}$	1330 ± 70
300		$(2.08 \pm 0.04) \times 10^{13}$	1429 ± 80
600		$(2.06 \pm 0.02) \times 10^{13}$	1698 ± 72

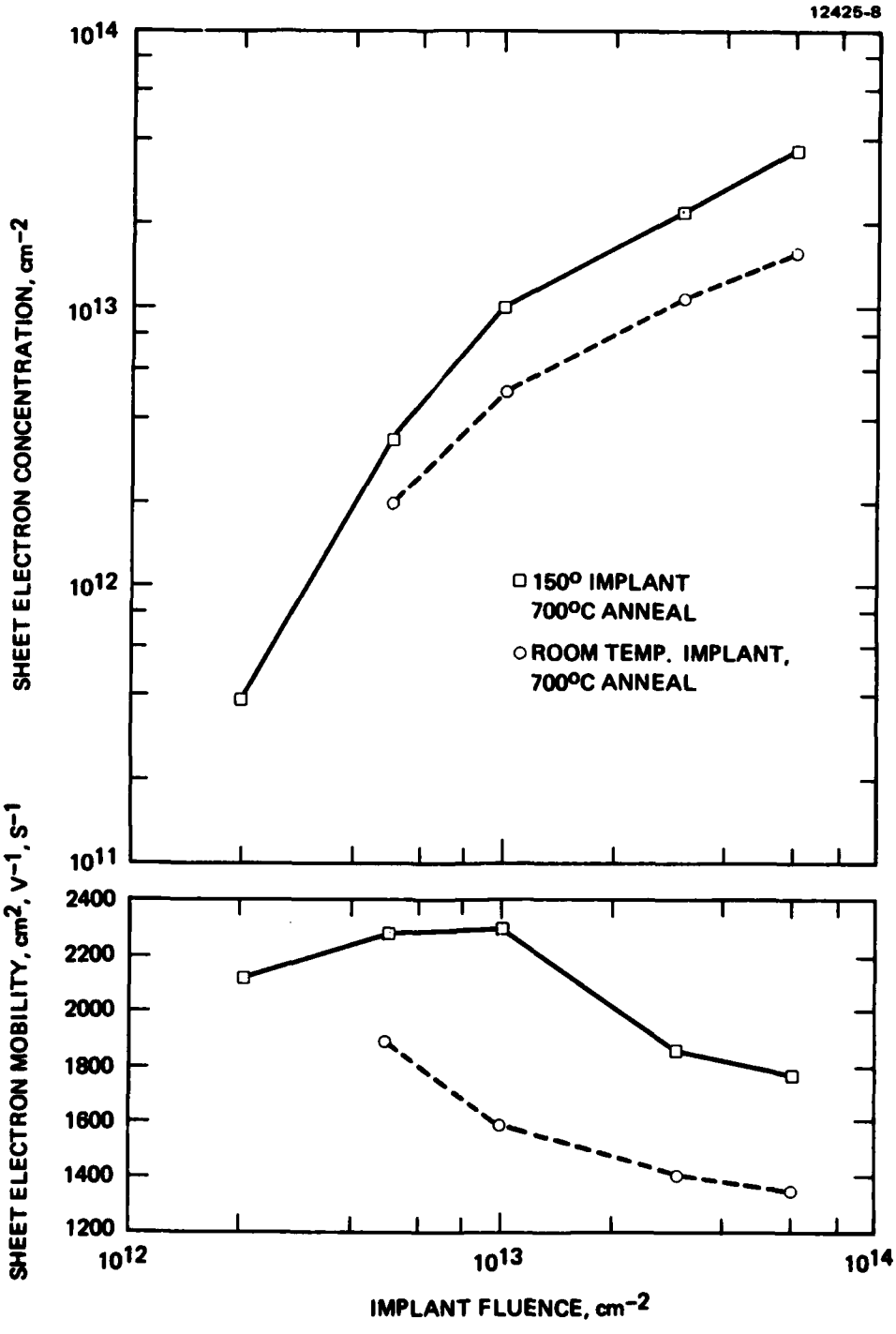

Figure 26. Variation of sheet electron concetration and mobility as a function of implantation dose from Se-implanted InP samples annealed with PSG encapsulant at temperatures shown.

SECTION 5

SUMMARY

The technical progress discussed in the preceding sections of this report is summarized below.

In the area of epitaxial growth, we have demonstrated that InP n-type epi-layers with carrier concentrations of 3×10^{15} and carrier mobilities of ~5,000 $cm^2\ V^{-1}s^{-1}$ can be grown reproducibly using the infinite solution growth technique. To grow layers with such desirable properties, it is necessary to maintain the growth solution in a controlled ambient consisting of 0.1 to 10 ppm of water vapor in hydrogen. Detailed electrical, optical and secondary ion mass spectrometry (SIMS) analysis of the grown layers have shown that in InP LPE layers silicon and sulphur are the major residual impurities. The presence of water vapor suppresses the reduction of quartz, and consequently, the incorporation of silicon in the epi-layers. Layers grown in the absence of water vapor show the presence of large concentrations of silicon.

We have identified the surface degradation of InP samples prior to epitaxial growth as a major problem in growing layers with device-quality morphology. To prevent such degradation, we have designed a sample holder which allows us to maintain InP substrates in an ambient of flowing dilute phosphine prior to epi-growth. This procedure will be particularly useful in the growth of lattice-matched InGaAs layers on InP substrates.

A major problem in the evaluation of bulk InP is the accurate determination of iron in InP. The thermal stability (i.e., the ability to maintain its semi-insulating character after a high temperature annealing treatment) of semi-insulating InP substrates is related to the concentration and the mobility of Fe in InP. During the next phase of this program, we will perform a variety of measurements to gain a better understanding of the behavior of Fe in InP.

In the area of ion implantation doping, we have established procedures for reliably annealing InP samples at high temperatures (650° to 750°C) using phosphosilicate glass as the encapsulant.

Electrical measurements on Be-implanted InP samples clearly demonstrate that efficient acceptor activation can be achieved following an anneal temperature as low as 550°C. At high concentrations (>7 x 10^{17} cm^{-3}) dramatic redistribution of the implanted dopant is observed in Be-implanted InP following high temperature annealing. This redistribution behavior will limit the highest acceptor concentration achievable in Be-implanted InP.

Among the donor dopants studied, silicon, germanium, tin, and selenium are well-behaved donors in InP. High percentage carrier activation with high electron mobilities can be achieved with these dopants in InP. In the case of the heavier mass dopants (Ge, Sn, and Se), and at high fluences, it appears that implantation at elevated temperatures (~150°C) is benficial and results in increased carrier activation and improved mobility in the implanted layers. Carbon appears to be an inefficient n-type dopant in InP among all group IV impurities. Low carrier activation with poor mobilities were observed in carbon-implanted and annealed samples.

END

FILMED

3-83

DTIC